

Single-Channel EEG Probe

A study on EEG signal acquisition and electrode performance

Diogo Antunes¹, Pedro Osório²

¹ Instituto Superior Técnico,
MSc Biomedical Engineering diogomdantunes@tecnico.ulisboa.pt
² Instituto Superior Técnico,
MSc Biomedical Engineering pedro.c.osorio@tecnico.ulisboa.pt

1 Introduction

The Electroencephalogram (EEG) signal is measured through the scalp and is produced by the brain's cortical electrical activity. This signal has several applications ranging from clinical uses like in monitoring the brain state for the study of cognitive processes and mental disorders to their use in Brain Computer Interface technologies. Traditionally the EEG acquisition systems are lab based, requiring a large number of electrodes that contact the scalp through a conductive gel and which are placed according to a standardised spatial configuration.

Despite providing the most noise free and extensive data, the current lab-grade approach to EEG acquisition is limited in terms of portability, mainly due to the large number of electrodes, and also in terms of subject comfort, due to the use of conductive gel at the electrodes and a skin preparation gel. For the same reasons, the setup process is also quite lengthy.

Developing an easier-to-use acquisition strategy, with faster setup times, increased portability and comfort would enable the use of EEG in several new contexts.

1.1 Physiological concepts

Before dwelling into the characterization of a typical EEG, it's important to understand the physiological phenomenon and mechanisms underlying the generation of the recorded potentials which compose the signal. This not only provides deeper insight and a wider view to the whole paradigm but can also be clinically relevant when interpreting certain situations, for instance, like convulsions or metabolic disorders of the brain [1].

Neurons and glial cells are the main constituents of the Central Nervous System. Neurons are composed of a cell body (soma) which branches out into axons or dendrites. These two structures are responsible for the communication with other cells or organs. The contact between two neurons is made through synapses, which is made between an axon and along the dendrites or the soma. Glial cells, in their turn, are located between neurons and are in contact with them but also blood vessels.

Synaptic activity in neuronal cells is responsible for changes in the cell's membrane potential, which has a resting magnitude between 60 and 70 mV. When an action potential is transmitted through a fiber two types of potentials can occur in the connecting neuron. If the synapse is excitatory, then an excitatory postsynaptic potential (EPSP) is generated, which summed with another EPSP gives rise to an action potential in the postsynaptic neuron. On the other hand, if it's an inhibitory postsynaptic potential (IPSP) it causes the target neuron's membrane to hyperpolarize. These fluctuations of the membrane potential are induced by ionic current flows between the cell's intra and extracellular spaces.

Glial cells' resting membrane potential is similar to neurons', however it doesn't suffer the same type of fluctuations, with no action or postsynaptic potentials being generated. But it does, however, suffer changes too.

They are sensible to extracellular potassium concentration, depolarizing when that concentration rises. This ensures functional connection to the surrounding neurons, which when are fired give lead to the increase of extracellular potassium, causing depolarization of the glial cells.

All these ionic current flows, mainly those arising from synaptic activity, contribute to the production of extracellular potentials called field potentials, which are the ones picked up by the EEG electrodes. The polarity of the potential and its shape depend on the kind of synapse involved (excitatory or inhibitory) and whether the superficial neuron is the one transmitting or being the recipient of the action potential. The field potentials can be classified into different types. EEG refers to the potentials recorded with a frequency limit around 100 Hz relative to a reference, which is electrically inactive, and with amplifier with a time constant of 1 second or even less. The called DC potentials are similar but recorded with a direct current amplifying recorder, which allows to capture lower frequencies, but are practically more difficult to realize.

However, the EEG signal is not composed of a single field potential, but several which originate the waves on the cerebral cortex which are superficially captured by the electrodes. These can be generated by afferent fibers which cause synchronous influxes towards the superficial structures, in which case high amplitude EEG waves are recorded. On the other hand, if the influx has a higher frequency and takes a longer time then the field potentials will have negative polarity and show small variations. The EEG waves will then be of reduced amplitude and higher frequency.

1.2 Conventional EEG recording

Although digital technology has drastically changed the way neurophysiological signals are processed, most of the instrumentation for signal acquisition remains analog. In this section we give a little bit of insight into how EEG activity is typically recorded.

First it is important to keep some considerations into mind, and one of them is that there are sources of noise which can highly affect an EEG signal recording. The electrical power supply current in a building can introduce a signal up to 10000 times larger than EEG in the human body in the form of a 50-60 Hz field. EMG, mainly due to eye movement, can also be a source of higher amplitude artifacts [1]. Such artifacts might be impossible to remove but some of the recording instrumentation used and processing techniques can be successful in attenuating them.

The electrodes are one of the main components of an EEG recording setup and they provide an interface between the human tissue and the wires which carry the current that is read as the signal. Conventionally, simply placing metallic conductive electrodes on the skin isn't an option due to the skin's tissue and oils insulating effect. An ionic solution abundant in chloride and sodium, and which can have a flowing form or even be in the form of a thick paste, is usually applied on the skin to increase conductivity. They normally have the shape of a cup and can be made from gold or be silver coated. The conventional disposable adhesive electrodes most often use a silver-silver chloride interface paired with a chloride solution, stemming the most stable neurophysiological electrode, with good low-frequency recording range and resistance to polarity.

In neurophysiological recording the amplifiers are of major importance and additionally to the gain, they must also have other desired characteristics: high common-mode rejection; linearity and flatness across frequency range; high input impedance. One of the challenges in EEG recording is the removal of the high amplitude fields caused by the electrical current supply. However, most of the electrical noise shows similar amplitude in close areas of the body. Such identical potentials are defined as common-mode signal and can be removed by simply subtracting the whole signal acquired by one electrode to the one acquired by another which results in what is called the differential-mode signal. In EEG recording several electrodes are used, which are also denominated as channels, and they all have a common single ground. This must not be mistaken with the reference used in referential EEG recording montages.

Regarding montages, the first standardized system, which is still the most widely used is the International 10-20 System. EEG activity varies notably depending on the acquisition location on the scalp, which lead to the use of multiple electrodes and channels. For comparative purposes it was also necessary to define standard method of data acquisition. This led to the development of the IS 10-20, a standardized electrode positioning system. It makes use of 21 electrodes and displays 16 channels [2].

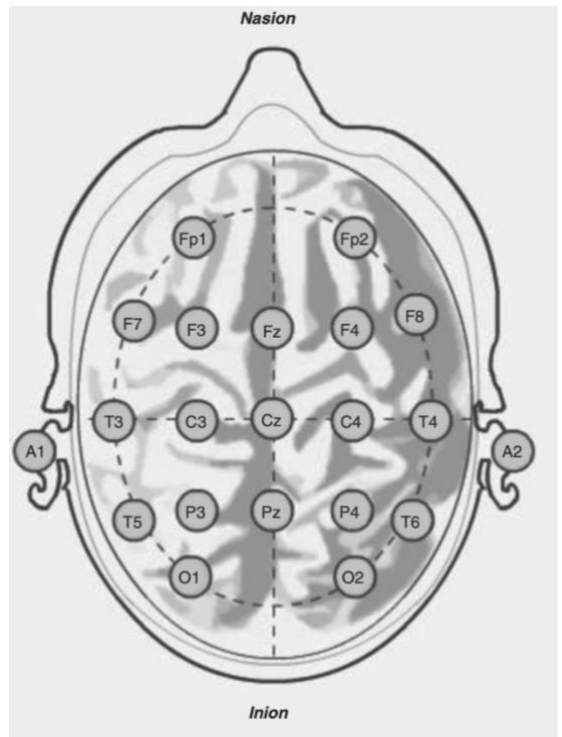


Figure 1 – Positions of the 19 scalp electrodes and two reference electrodes according to IS 10-20. Adapted from [2].

1.3 Normal EEG in adults

Classifying a recording as a normal EEG might not be a simple task since there isn't a clear form or distinctive characteristic that the wave must have in order to be called so. Some use the absence of abnormalities as the classifying factor. However, there are patterns common to all healthy individuals that have been identified over the years. Rhythm is an important aspect of the EEG signal, which has a wide spectral range between 0.1 and 100 Hz, but in adults can be restricted to 0.3 to 70 Hz. The spectrum is divided in bands which have clinical relevance: Delta which comprise frequencies up to 3.5 Hz; Theta from 4 to 7.5 Hz; Alpha from 8 to 13 Hz; Beta from 13 to 30 Hz; Gamma above 30 Hz. The EEG signal can also be described by its amplitude. The cortical potentials can show magnitudes from 500 to 1500 μ V, however due to attenuating effects of tissues like the bone, cerebrospinal fluid or even the skin of the scalp the superficial recording have a much lower range from 10 to 100 μ V [1].

1.3.1 Alpha band

The alpha band includes the frequencies between 8 and 13 Hz, and is seen during a conscious state, with the term wakefulness being normally employed such state. The closure of the eyes and physical relaxation of the body increases their prominence, which is reduced in attentive states, mainly visual. Regarding their shape, they usually present sinusoidal rounded waveforms. Their generation is still not entirely comprehended, but it is believed that they have cortical origin with corticocortical and thalamocortical systems having a role. They are, however, undoubtedly, a demonstration of posterior brain activity being most visible parietal, occipital and posterior temporal sections of the head. This type of activity is closely related to a relaxed wakeful state, and it becomes less prominent in anxious and attentive states, as well as in sleep.

1.3.2 Beta band

Beta comprises the frequencies between 13 and 30 Hz. It can be seen along the different regions of the brain, however rhythmical activity is most commonly found in frontal and central locations. Motor activity and tactile stimulation are known to cause attenuation, while the administration of sedatives or tranquilizers leads to an increase of the activity.

1.3.3 Theta band

The theta band is used to denote the frequencies between 4 and 7.5 Hz. It is presumed to have thalamic origin, hence its name. Recordings from a normal awake adult have little amounts of this band and no clear rhythmicity in these frequencies. Increased volumes of activity can be indicative of pathology. This type of activity has been found to be related to cholinergic activities stemming from central cholinergic pathways. Tasks requiring mental effort such as problem solving have been shown to be correlated to rhythmic activity in the 6 to 7 Hz band.

1.4 Epilepsy and EEG

One of the most, if not the most, clinically relevant context where EEG is used is in epilepsy. It is successful not only in diagnosing if a patient suffers from it, but also in localizing it spatially in the head and also in monitoring and evaluating therapeutic procedures.

The so-called interictal epileptiform discharges (IEDs) are used to identify epileptic attacks and can several forms: spikes, sharp waves, spike-wave complexes, polyspikes, or seizure patterns, among others.

A spike is a transient with visible distinction from background activity, with typically a negative main component and duration ranging from 20 to 70 milliseconds. It is normally distinguished from background activity due to its clearly higher amplitude, but in cases where it is similar the shorter duration can give it away. Although there are common characteristics, inter and intrapersonal differences exist as well as between spikes from the same recording. They are hypersynchronous events that occur due to excessive neuronal firing. Single spikes usually display multiphasic nature with the sequence of a minor positive, followed by a major negative and again a minor positive component being the most common. In Figure 2 we can observe various EEG recordings displaying spike structures.

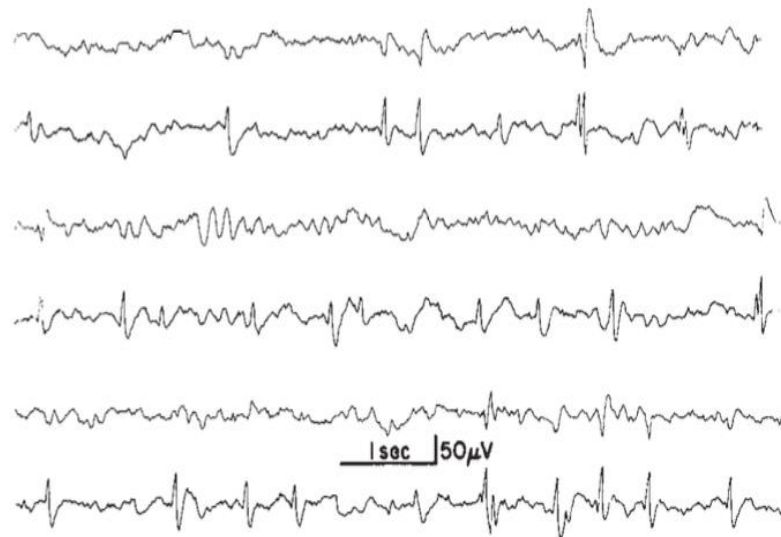


Figure 2 – EEG recordings displaying different spike morphologies recorded in a 6 year-old patient. Adapted from [1].

Sharp waves are another common form of epileptic discharges visible in EEG. A sharp wave is defined as a transient with visible distinction from background activity, with duration ranging from 70 to 200 milliseconds. They distinguish themselves from spikes not only in their duration but also in their morphology. While the rising phase is similar to spikes, the descending is more prolonged. Like spikes they are epileptiform discharges and a signal of epileptic seizure, however in some patients without history of seizures they might also appear.

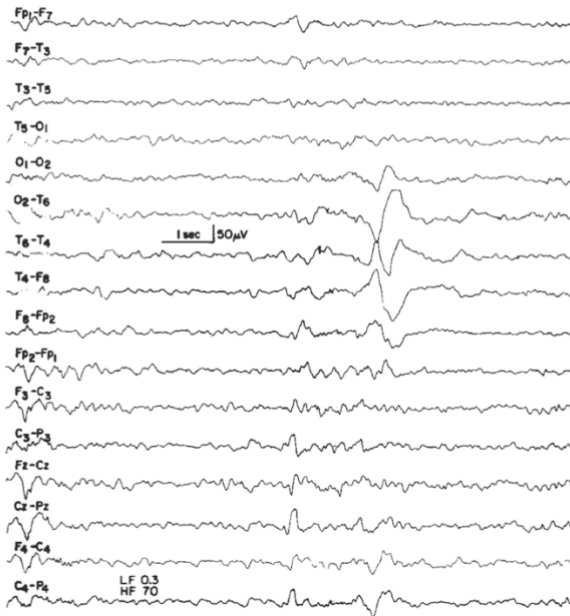


Figure 3 - EEG recordings displaying very slow sharp waves recorded in a 6 year-old patient. Adapted from [1].

1.5 Current alternatives to lab grade instrumentation

With the growing developments in technology and electronics, mainly in signal recording and processing, over the years it has been possible to develop portable systems for EEG acquisition. Most of the efforts have been made towards wearable and wireless systems. However, the development of reliable dry electrodes has widened the applicability of EEG technology to situations where conductive gel and wired setups might cause constraint. Wet electrodes require the application of a thick paste or gel to increase conductivity which some patients can see as a source of discomfort, as well as the time needed for the cleaning of the skin afterwards can be impractical. So, although most wearable devices still use wet electrodes, there are growingly appearing dry electrode systems some even commercially available currently [3][4][5].

One of them is *myBrain*, developed by Universidade do Minho. The system is composed of an electrode cap incorporated into a hat, to which the circuit board and batteries are also attached. It uses 32 dry electrodes which have a pin contact interface configuration. The contact with the scalp is made by 32 spring-loaded pins in each electrode. The software includes an epileptic event detection algorithm [6].

Another example is the *Melomind* headset manufactured by myBrain Technologies. This is an interesting device to its contrasting design relative to the other available systems. It is a neurofeedback headset which contains detachable dry electrodes (as visible in Figure 4).

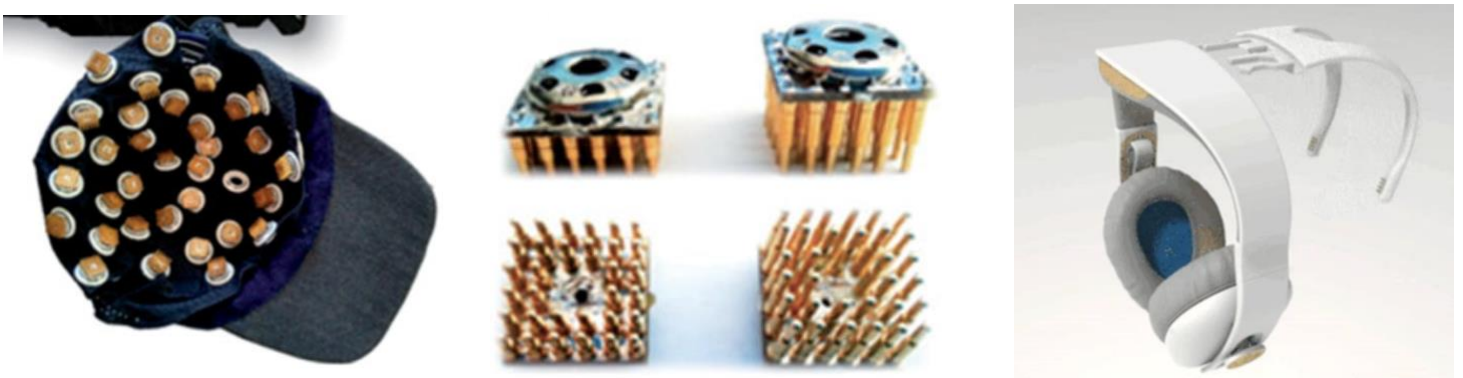


Figure 4 – *myBrain* incorporated electrode cap to hat (Left). 32 spring-loaded pin electrodes used in *myBrain* (Center). *Melomind* headset with detachable electrodes (Right).

1.6 Proposed solution

In this work, we set out to develop a dry electrode single-channel EEG handheld probe, which makes use of a monopolar configuration. This differs from the majority of the current systems in the sense that it isn't a fixed wearable device, which can introduce some difficulties. The contact of the electrode with the scalp is determinant to the acquired signal's quality, and it can be compromised by lack of stability that a handheld system can be susceptible to.

The use of monopolar recording can also be source of some limitations. Practically it is clearly advantageous, with the requirement of a single electrode doing the signal recording, and another placed on a low activity region such as the mastoid. In bipolar recording the two lead electrodes can detect signals that have overlapping in-phase information, which can lead to them cancelling each other out in the final differential signal. In this case a monopolar setup would lead to more accurate results. However, at the same time, the noise common to both electrodes would also be cancelled, which is in itself a type of filtering, whereby noise can heavily distort monopolar recordings [7].

One option explored was also the design of 3D printed electrodes dry electrodes to be incorporated into the probe. The vantages, other than the ones already discussed for dry electrodes in general, would also be the ease of manufacturing and cost that such a DIY and home-made solution implies. However, dry electrodes can suffer from poor contact noise and their design is key in their success. The idea was to design dry comb electrodes that could penetrate the hair for easier contact with the scalp.

As previously discussed, the diagnose of epilepsy and identification of seizures are some of the main clinical applications of EEG. The development of such a device that is here proposed would yield a significant contribution to this paradigm since it would enable preclinical evaluation, in the context of a waiting room, of patients' brain activity. The acquisition of a good enough quality signal in which abnormalities and the characteristic structures of the epileptic signal can be identified is then the goal.

2 Methods

2.1 Equipment and Setup

2.1.1 Overview of the Montage

The acquisition of the EEG signal is made possible through the pipeline depicted in Figure 5.

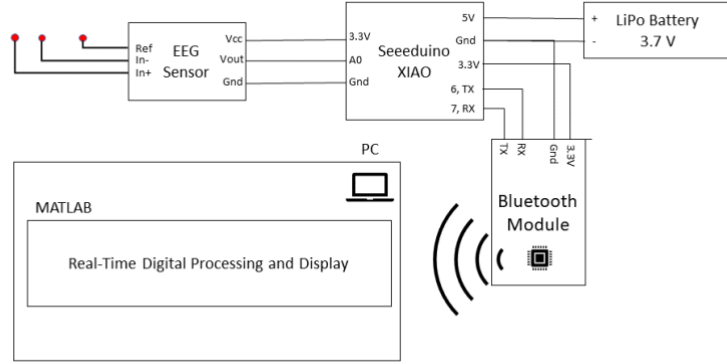


Figure 5 – Scheme of our approach for a single-channel EEG acquisition system with real-time processing.

A set of electrodes are used to collect signal from specific locations of the subject's scalp. The various electrodes are connected to an EEG sensor, which outputs a single channel raw EEG signal through the analog pin V_{out} . This output pin is connected to an analog pin of the Seeeduino XIAO, which enables us to sample the the analog signal into digital codes (10-bit ADC) and redirect them to a Bluetooth module [8] via the XIAO's TX pin. When a computer is paired with this module, the data reaching the latter is broadcasted to the respective PC Bluetooth Communication Port. At this point, we can use a MATLAB script to access the PC's Communication Port and store the samples of the EEG signal being printed onto it by the module. The sampling rate is defined in the Arduino code executed by the XIAO and in this case was specified to 250 Hz, which is well above twice the highest relevant EEG frequency. The Arduino code and the MATLAB files were all delivered alongside this report.

Once the data is being received by the computer, we can process a user-specified window of the signal, extract its features, and plot it at a user-specified frequency.

Finally, a LiPo 3.7V rechargeable battery is used to power the XIAO via the 5V pin, which, in turn, will power both the sensor and the Bluetooth module via the 3.3V pin.

2.1.2 EEG Sensor

As we have stated before, the EEG signal has low amplitude ($1\text{-}100\mu\text{V}$) therefore requiring a large amplification in order to be digitally processed and visualised.

With that in mind, an essential component in our acquisition system is the EEG sensor. This piece will work as differential amplifier and must have several characteristics in order to perform adequately.

Firstly, this sensor's internal filters must be tailored in such a way that it provides attenuation to frequencies outside the EEG frequency band. Since the EEG most relevant frequencies are from 1 Hz to 40 Hz, the sensor's measuring bandwidth must at least include this frequency interval.

Being a differential amplifier, the sensor must eliminate or attenuate common mode voltage between the signals collected from different electrodes. This process is very determining of the measured EEG's quality, as it allows the attenuation of the noise common in all channels like the electromagnetic interference at 50 Hz stemming from the electrical distribution. The ability of a differential amplifier to attenuate common mode signals is measured by the Common Mode Rejection Ratio (CMRR) and its common values in commercial EEG amplifiers are between 100 to 110 dB.

Another important characteristic to consider when selecting the EEG sensor is the input impedance. Given the already low amplitude of EEG signal, we must have a system with the largest possible input impedance to minimize its further attenuation. In fact, since in this case we are aiming to create a dry electrode acquisition

system, with larger electrode impedances this parameter is of added importance. According to Mettingvrijn et al., 1991[9], the input impedance should be at least 100 times large the electrode impedance.

Considering all these factors we decided to employ the BITalino's EEG sensor [10]. This board provides a 100 dB CMRR, input impedance larger than $100\text{G}\Omega$ and a bandwidth of 0.8 to 48 Hz hence being a good choice for our application. It stands on a value of 37.5€.

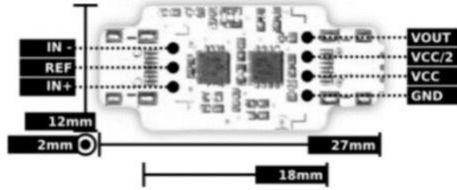


Figure 6 – BITalino's EEG sensor pinout and dimensions [10].

This sensor has 3 input pins allowing a bipolar configuration with two measurement electrodes (In^+ and In^-) detecting scalp potentials between them with respect to a reference one (Ref). It is however possible to transform this configuration into monopolar as we will see in later sections.

The analog output signal can be obtained at pin V_{out} and sampled into digital codes by an ADC like the one in the Seeeduino XIAO. We can retrieve the real values of the EEG signal in μV based on the sensor's gain ($G=41782$), the number of bits of the ADC used and the sensor's operating voltage (V_{cc}) (see Equation 1).

$$\text{EEG}(\mu\text{V}) = \frac{\left(\frac{\text{Digital Code}}{2^n} - \frac{1}{2} \right) \times V_{\text{cc}}}{G} \times 10^6 \quad (1)$$

2.1.3 Electrodes

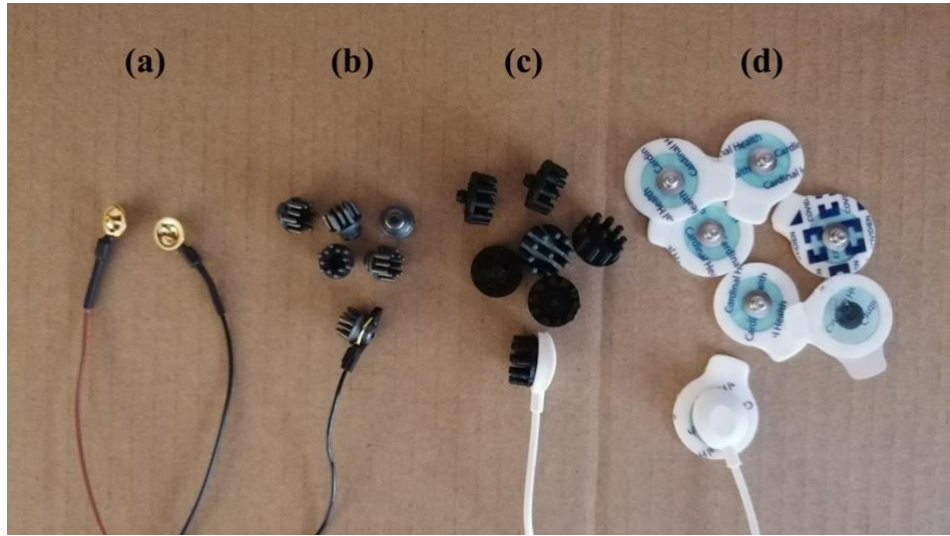


Figure 7 – Every electrode used throughout this project. (a) Gold cup electrodes; (b) Dry comb Ag-AgCl coated electrodes; (c) Dry comb electrodes 3D printed with a conductive PLA; (d) adhesive gelled disposable Ag-AgCl surface electrode (H124SG).

In order to converge on the most suitable electrodes for our final device we set out to perform acquisitions with multiple types. In total we tested 4 types of electrodes, ones which are depicted in Figure 7.

Starting by the wet electrodes, we experimented with gold cup electrodes from Florida Research Instruments Inc. [11] and adhesive gelled disposable Ag-AgCl surface electrode (H124SG) from Covidien Kendall [12].

The gold cup electrodes are used simultaneously with conductive gel [13] which provides a lower contact impedance, fixation while also acting as a mechanical buffer maintaining contact with skin during movement. Despite its excellent conductive properties, it is quite expensive and uncomfortable for the test subject.

The H124SG electrodes have a pre-gelled adhesive side that provides fixation and low contact impedance while also having snap-on connectors on the other side, allowing for an easy connection to the lead. Given the inherent fixation and comfortability of these electrodes we decided to use them as the fixed reference in most of our acquisitions. Contrarily to the previous electrode this option is very inexpensive.

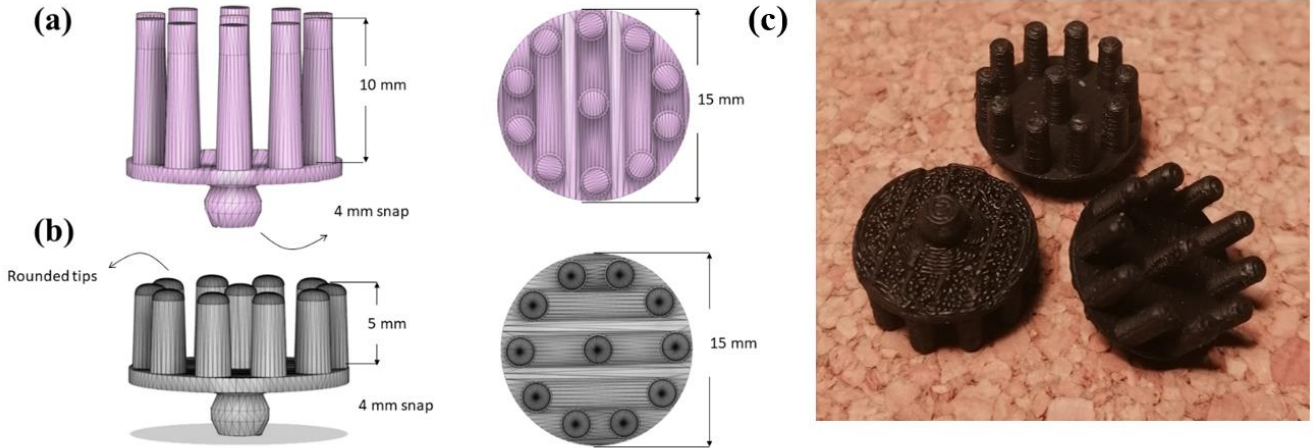


Figure 8 – (a) Original electrode design from [4]; (b) Our final design; (c) 3D printed electrodes.

We experimented with electrodes that were 3D printed with an electrically conductive polymer (Proto-pasta Conductive PLA [14]). The design used was based on one from [4], but, since it was originally made for a 3D printed electrode with a conductive coating, we altered it to be more suitable for our application. The adjustments consisted of reducing the length of the spikes to minimize its resistivity and rounding its tips for a better hair penetration. Note that this design includes a 4mm snap that is compatible with the same snap-on connector cables used for the H124SG electrodes. We can see the design features in Figure 8.

From the polymer's manufacturer website [14] we get that the volume resistivity of a 3D printed part along its vertical axis should be $115 \Omega\text{-cm}$, meaning that a 1cm side cube has a resistance of 115Ω . We tried to measure the resistivity of our electrodes with a multimeter, but the value obtained did not stabilise, always varying from $1k\Omega$ to $2k\Omega$. The electrode design makes it difficult to evaluate its resistance with the conventional multimeter's leads due to unstable contact. Even though we were not able to measure a fixed value, we can safely say that the real electrode's resistance is not larger than $2k\Omega$ hence being within acceptable values for EEG acquisition ($<5k\Omega$) [15]. The designs were edited in Autodesk's Fusion 360 software and the printing was executed by a SnapMaker 1.0.

Another dry electrode that we experimented with was the dry comb Ag-AgCl coated electrodes that we had shipped from Florida Research Instruments Inc. [16]. This model's pin length is the same as the previous one, but the diameter of each pin is much smaller, therefore we expect to achieve a better penetration through hair with this model. Adding to that, since this electrode has a conductive Ag-AgCl coating it offers a much lower resistance to electrical current (generally under 1Ω [4]).

Table 1 - Cost related to each type of electrode.

Type	Cost (€)	Observation
Gold Cup Electrode	5.09	Includes lead. Cost would be slightly larger if considering the conductive paste
H124SG Electrode	0.33	Price per unit when bought in a 50 pack
Proto-pasta Conductive PLA (50g)	9.57	Allows for a significant amount of 3D printed electrodes
Dry Comb Ag-AgCl coating + Lead	7.27	The respective lead is the most expensive at 6.70€ per unit. The electrode is only 0.57€

2.1.4 Monopolar and Bipolar Configuration

It is within the scope of our study to explore how the different configurations of EEG data acquisition could influence the final signal. Despite the sensor we used being designed for a bipolar acquisition, we could obtain a monopolar configuration by simply making sure that both the In- and Ref pins receive the same signal. This was achieved by simply soldering the cables connected to these two pins in a way that we can use only one electrode, as depicted in the figure below.

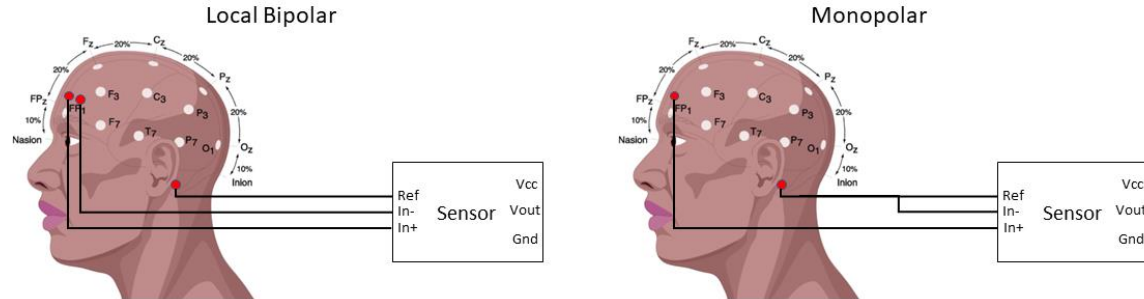


Figure 9 – Local Bipolar Configuration and Monopolar configuration.

In a bipolar acquisition the distance between the two lead electrodes can influence the type of signal collected. The sensor's documentation [10] specified that it was designed for a local bipolar acquisition, where both leads are located close to each other allowing the measurement of differences of the voltage potentials within a specific region of the scalp. In our experiments we then compared the signal obtained through this local bipolar configuration with the one from a monopolar configuration, with respect to noise susceptibility and the signal morphology.

The configurations we tested are presented in the figure below, where the first 3 sets of cables correspond to monopolar configurations while the bottom one is bipolar. Among the monopolar acquisition systems, we tested one using gold cup electrodes (a), one using dry comb Ag-AgCl coated electrodes for the lead and an adhesive gelled disposable Ag-AgCl surface (H124SG) electrode for the reference (b). This reference electrode was also used in an additional monopolar configuration with two snap-on connectors (c), where the lead can either be our 3D printed electrode or also the H124SG. Regarding the bipolar acquisition systems, the one presented below has snap-on connectors in all three cables (d), allowing a configuration with all H124SG electrodes and also a mixed montage of H124SG as the reference electrode and our 3D printed

below, we also tested a bipolar configuration with dry comb Ag-AgCl coated electrodes as leads and a H124SG electrode as reference.

Note that the configurations that we tested all rely on an adhesive electrode for reference, it being a gold cup electrode fixed with conductive paste or an adhesive H124SG electrode. Since the reference electrode was always located in the subject's mastoid, where the fixation of dry electrodes is quite difficult, we opted to use ones that could be easily attached, minimising movement during acquisitions, hence reducing the noise.

An elastic band was used in every configuration but the gold cup, to provide fixation to the dry electrodes and a better electrode scalp interface in the H124SG electrodes.

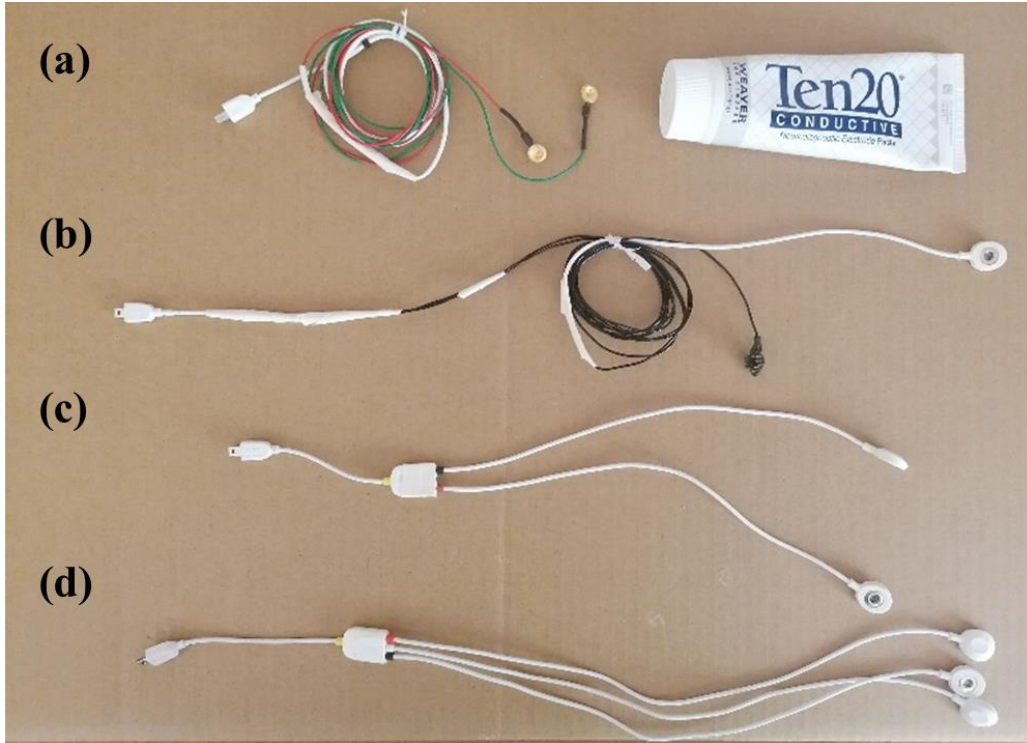


Figure 10 - Configurations used to acquire EEG signal. (a) Full gold cup monopolar montage with the required conductive paste; (b) Mixed monopolar montage with dry comb Ag-AgCl lead and a H124SG reference; (c) Monopolar cable configuration with snap-on connectors allowing the attachment of both H124SG and 3D printed electrodes; (d) Bipolar cable configuration with snap-on connectors allowing the attachment of both H124SG and 3D printed electrodes

2.1.5 Probe

The final objective of this study is to develop a prototype of an EEG probe that would enable us to easily change the location of the acquisition, allowing assessment of various scalp regions with a reduced number of electrodes.

In sections to come, we will present our experimental protocol, describing the rationing behind the selection of the most suitable electrodes and configuration for our final solution. In this section we will describe the design of the probe used to house these electrodes.

As we will later explain, we found the best configuration for our EEG probe to be a mixed monopolar montage with a fixed wet reference and a dry lead, leaving us with the task to develop a probe that could house both types of dry electrodes that we wanted to test.

We used a simple design based on a UHU glue stick allowing the coupling of our 3D printed electrode's lead at one end and the dry comb Ag-AgCl coated electrode's lead at the other. The 3D printed electrode's lead is attached to the tube's body at the rotating end as it has the perfect radius for the lead's head to fit in while also

being tight enough to keep it in place. We only needed to make a small cut to allow the exit of the cable (Figure 11b). To attach the dry comb Ag-AgCl coated electrode at the other end we cut a small portion of the tube's wall to accommodate one extremity of the cable's head and made a hole on the opposite side of the tube using a soldering iron where the other extremity of the head could fit in (Figure 11e). A small piece of tape is then used to keep the electrode in place.

Considering the use of a dry comb Ag-AgCl electrodes, a wet adhesive electrode and a UHU glue tube we amount to a cost of approximately 10€ just for the probe. When including the EEG sensor, the battery and Bluetooth module we amount to an additional value of about 50€ (37,5€ + ~5€ + ~8€, respectively).

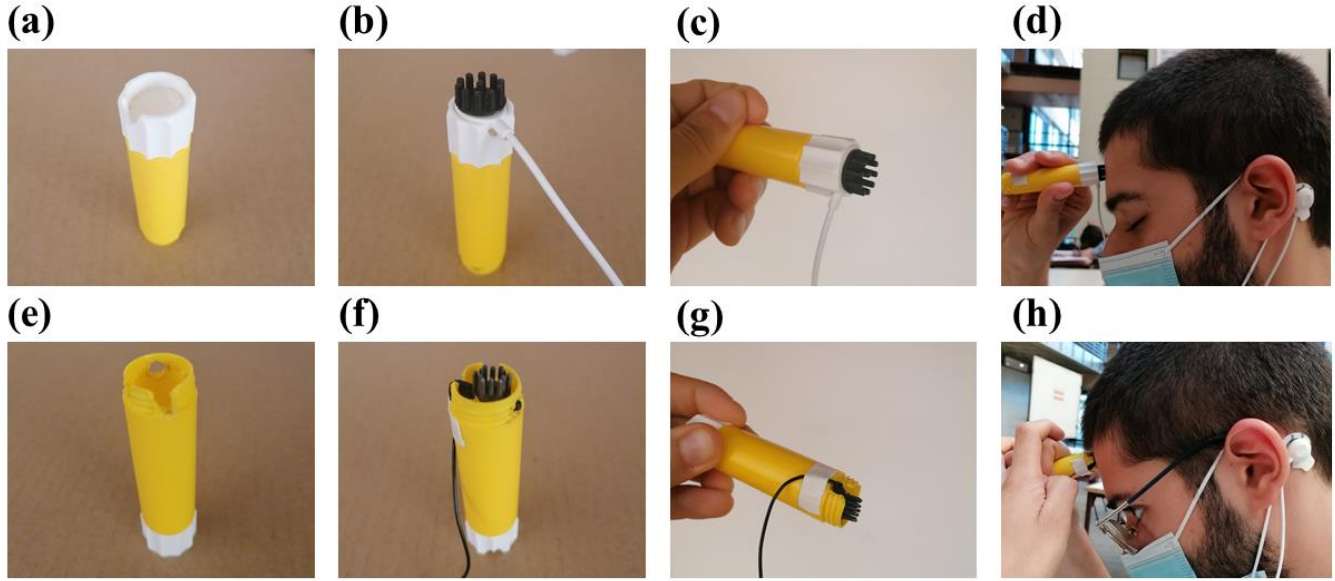


Figure 11 – Our basic prototype for an EEG probe capable of housing 2 different types of electrodes. Depiction of its various features and mode of usage.

2.1.6 Real Time Signal Processing

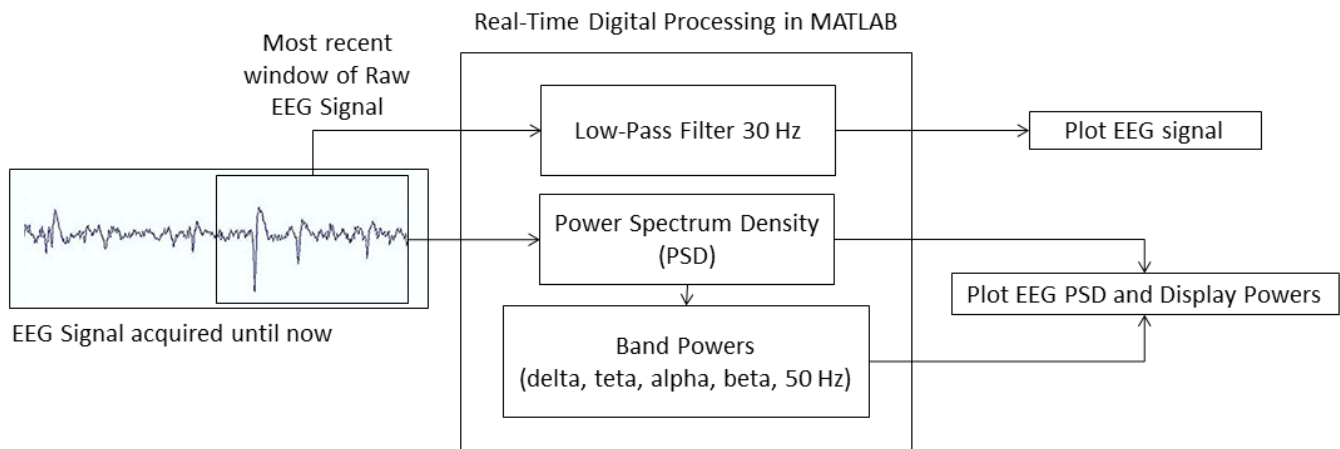


Figure 12 – Real time processing and display pipeline employed during our acquisitions.

As we have previously stated, the data coming from the sensor is sampled into digital codes by the XIAO's 10-bit ADC and broadcasted to the computer's Bluetooth Communication Port at 250 Hz.

We developed a MATLAB script (*Main.m*) that detects every time a new value is printed onto a user-specified communication port and runs a specific function. We created a function for this purpose (*callbackserial.m*) that stores the last printed value and, from time to time, processes a window of the EEG signal and displays various features. The length of the window and the frequency of the processing and display can all be specified by the user in the *Main.m* script.

The processing done during our acquisitions was twofold, providing both time and frequency information. Regarding the time information, we low pass filter at 30 Hz and plot the most recent 5 second window of our signal every 4 seconds, providing a continuous tracking of the evolution of our waveform. When it comes to the frequency information, we computed the Power Density Spectrum (PDS) of the last 5 second window also at the same rate. Adding to that, the relative band powers are also computed and displayed alongside with the PDS plot. Our processing steps are summarised in Figure 12.

One relevant feature of our processing is the computation of the power at 50 Hz, which is the line noise frequency. From that value the user can have an idea of the level of EMF noise corruption present in the signal being acquired and move to other locations if necessary. Note that for a good quality and full recovery of the EEG signal the line noise frequency power should not be larger than 40 dB (see Figures 13 and 14).

The low pass filtering was done using a 6th order Butterworth filter with zero phase. The PDS is estimated through the Welch's method using a 1 second window and 32768 DFT points, and the band powers are obtained by the integration of the PDS curve in each band of interest (Delta (1-3 Hz), Theta (3-7.5 Hz), Alpha (7.5-13 Hz) and Beta (13-29 Hz)). The relative band powers were computed by dividing each individual band power by the sum of the power across all relevant bands.

Note that we must have in mind the computational complexity of the processing procedure to be made in between displays when defining the display frequency and window length. We must certify that the processing and plotting can be made within the period between each display to guarantee a smooth tracking of the EEG activity. With the abovementioned processing, the plotting duration was within the interval of 0.2 seconds to 1.9 seconds, with the largest duration corresponding to the first display which is when the plot has to be initially generated. We could therefore safely push the period between displays down to 2 seconds.

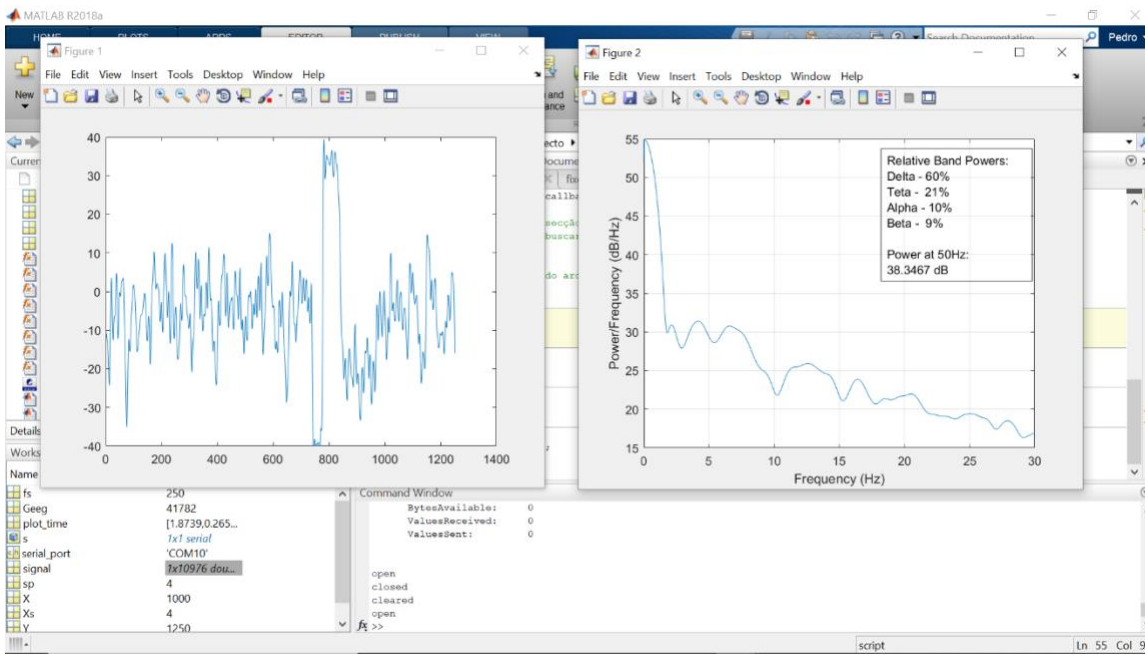


Figure 13 – Display of EEG waveform along with its spectrum. Acquisition made at a site with minimum noise, 38 dB/Hz.

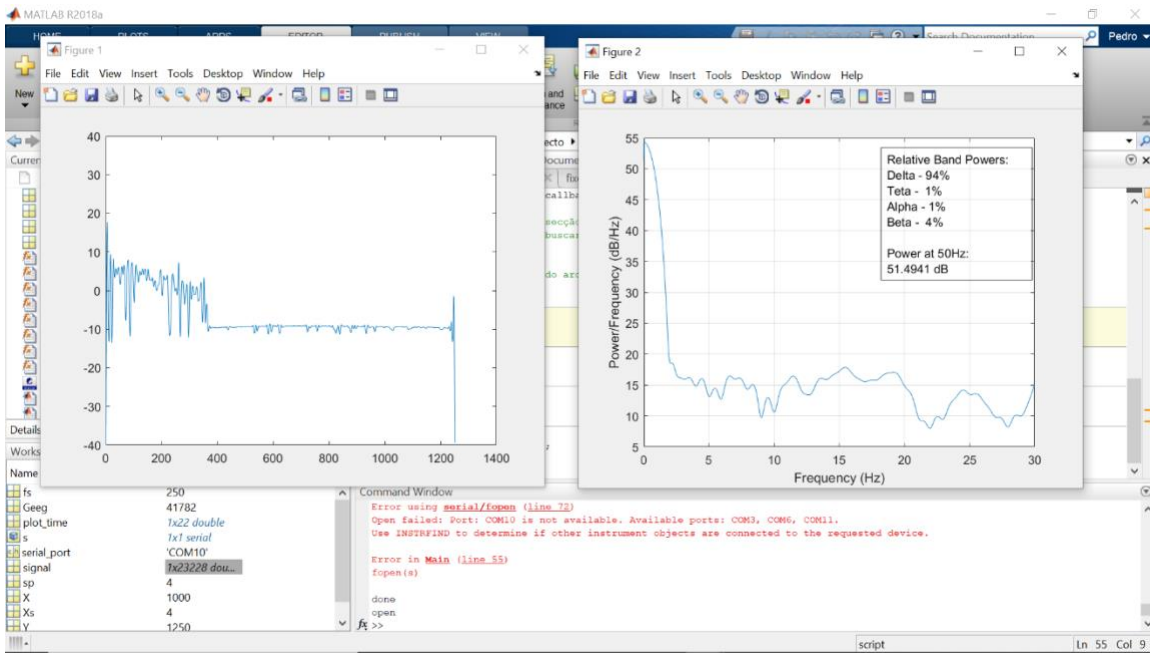


Figure 14 - Display of EEG waveform along with its spectrum. Acquisition made at a site with too much line interference, 51 dB/Hz

2.2 Experimental Protocol

We devised an experimental protocol to test multiple electrodes and acquisition configurations in order to evaluate their overall performance and suitability for our final application.

Two subjects, the authors of this work, male and with the age of 22 years were submitted to the protocol. This consisted in a series of measurements where the subjects remained as still and quiet as possible, considering the specific situation, over a period of two or more minutes while the EEG signal was acquired, with real-time signal plot and power density spectrum being displayed in the processing interface, which consisted in a personal computer laptop. The measurements were done in three different situations: eyes open, eyes closed and during cognitive load. These should yield different results regarding the spectrum's distribution. For instance, in a more relaxed and resting state with the eyes closed there should be a visible rise in the alpha band's density relative to a more focused and with the eyes opened situation. Whereas during a task of heavier cognitive load there should be a visible increase in beta band density relative to the other two. The cognitive load test consisted in the use of a mobile phone application which submitted the subjects to mental calculus effort.

It is also important to note that the acquisitions were made in two different rooms: one with reduced power supplies and electrical appliances to reduce corruption in the results due to electrical distribution noise; and another with a higher degree of interference by the power supplies.

2.2.1 Monopolar vs Bipolar Configuration

At a starting stage we explored how a monopolar acquisition would differ from a local bipolar one, mainly regarding noise susceptibility and signal morphology. For the bipolar acquisition three different setups were used: one with the conventional wet adhesive electrodes both as leads and reference; one with two dry comb AgCl coated electrodes as leads and an adhesive as reference; and one with two 3D printed electrodes as the leads and a conventional wet adhesive as the reference electrode. The respective monopolar configurations were also tested in order to be comparable. Another configuration was tested, which consisted in a monopolar one with a gold cup electrode as the lead and a gold cup electrode as the reference. However, this wasn't converted to a bipolar setup due to the practical limitation of having limited cables and electrodes for this type.

The mastoid, either right or left, was the chosen region for the reference electrode placement not only because it's an easy area to fixate it but also because it exhibits reduced activity (the electrode is mostly over bone tissue). The leads were placed on the forehead with a headband placed over them for fixation of the dry electrodes or enhancement for the wet adhesive ones. The obtained results lead us to choose a monopolar configuration as the desired ones for the probe.

2.2.2 Fixed Configuration Acquisition

Having chosen the monopolar configuration, the next step was to assess which was the most suitable type of electrodes. The goal was to design a probe with dry electrodes in order to reduce practical constraints, so the choice lied on the two options we had available: the dry comb AgCl coated electrodes manufactured by FRI and our own 3D printed dry comb electrodes. However, the gold cup and conventional adhesive setups were also tested to compare and test the quality of the signal obtained with the dry ones.

2.2.3 Hand-held Probe Acquisition

The final step of the development of our solution was the actual implementation of the probe. Due to time restrictions, it was not possible to obtain a more sophisticated design, for which a more rudimentary solution was found. Then we proceeded to test the probe with the performance of more acquisitions in the same conditions as previously described.

3 Results

3.1 Monopolar vs Bipolar Configuration

Noise susceptibility

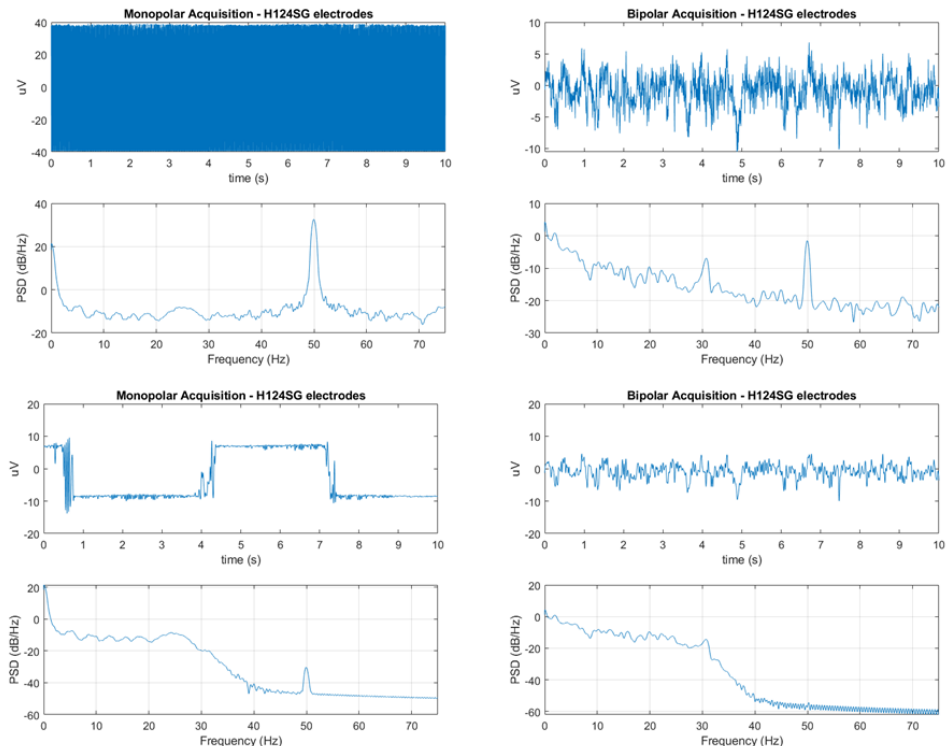


Figure 15 - Ten second windows of unfiltered (top) and filtered (bottom) EEG signals and respective PDS acquired with monopolar and bipolar configurations and with H124SG electrodes.

We started by analysing how bipolar and monopolar acquisitions systems would fair in a room with significant electromagnetic interference at 50 Hz. For that purpose, we performed acquisitions in such environment with a full H124SG electrode montage, both monopolar and bipolar. We can observe in Figure 15 the unfiltered EEG signals obtained in each situation, with reference at the mastoid and the leads located at the upper forehead (Fp1 in 10–20 placement system).

It is then quite clear that the monopolar configuration is quite more susceptible to noise than their bipolar equivalents as the peak of the PSD at 50 Hz is much more pronounced in the left plot than in the one at the right. The sturdiness of the bipolar configuration when dealing with this noise might come as result of the fact that in these acquisitions the two leads are located close to each other thereby detecting more similar noise which leads to a more successful common mode rejection of the latter. The same differential amplification does not provide such a good noise attenuation in monopolar acquisitions as the reference and lead electrodes are in different location of the head, with noise that is less similar between them.

Most of the times we can still extract features from the corrupted signals through filtering, however, when there is severe noise corruption, the retrieval of relevant biological data is not possible. This is what happens in this last monopolar acquisition as the filtered signal does not resemble EEG.

To further illustrate this phenomenon let us consider an acquisition at the same environment as before but with a full gold cup electrode monopolar configuration (Figure 16). In this case we can see that an increase in the noise intensity leads to a more extensive corruption and consequent EEG irretrievability. While a PC close to the acquisition site is not charging, the filtered signal is still recognisable as EEG, but as soon as we connect the charging cable the noise created by the flow of electrical current to said PC corrupts the measured signal to a point where even with low pass filtering it is not possible to retrieve the biological data. In Figure 16 we can clearly see in the right plots how the EEG becomes corrupted every time the PC is plugged in and regains its form after the PC is plugged off. Note that we started the acquisition without the PC charging.

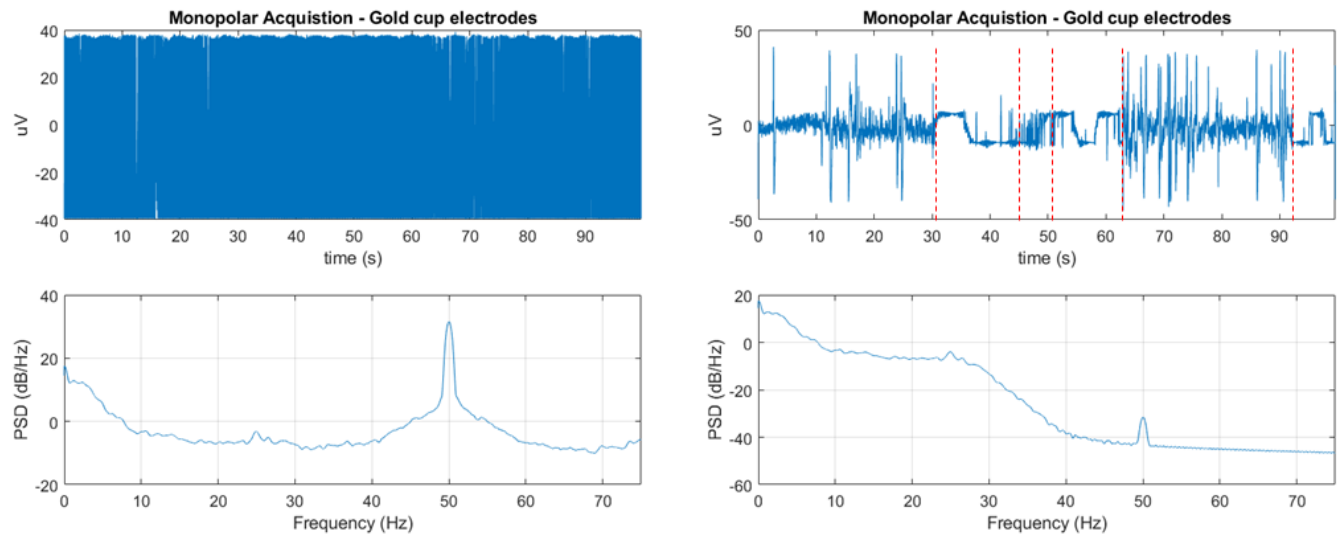


Figure 16 - EEG signal and respective PDS acquired with a monopolar gold cup configuration. At the left there is the unfiltered signal while at the right there is the low pass filtered signal at 30 Hz and its PDS. The red lines represent the moments when a nearby computer was plugged in or unplugged off the power.

Alpha peak detection

In order to decide the best approach for our final solution we also compared the performance of monopolar and bipolar configurations in locations where the noise from the electrical distribution was less significant, meaning a minimum number of power supplies and lighting units in the surroundings.

We then proceeded to perform acquisitions with both monopolar and bipolar configurations in both eyes open (EO) and eyes closed (EC) states to see if we could detect the well documented increase in alpha power from the former state to the latter in both configurations.

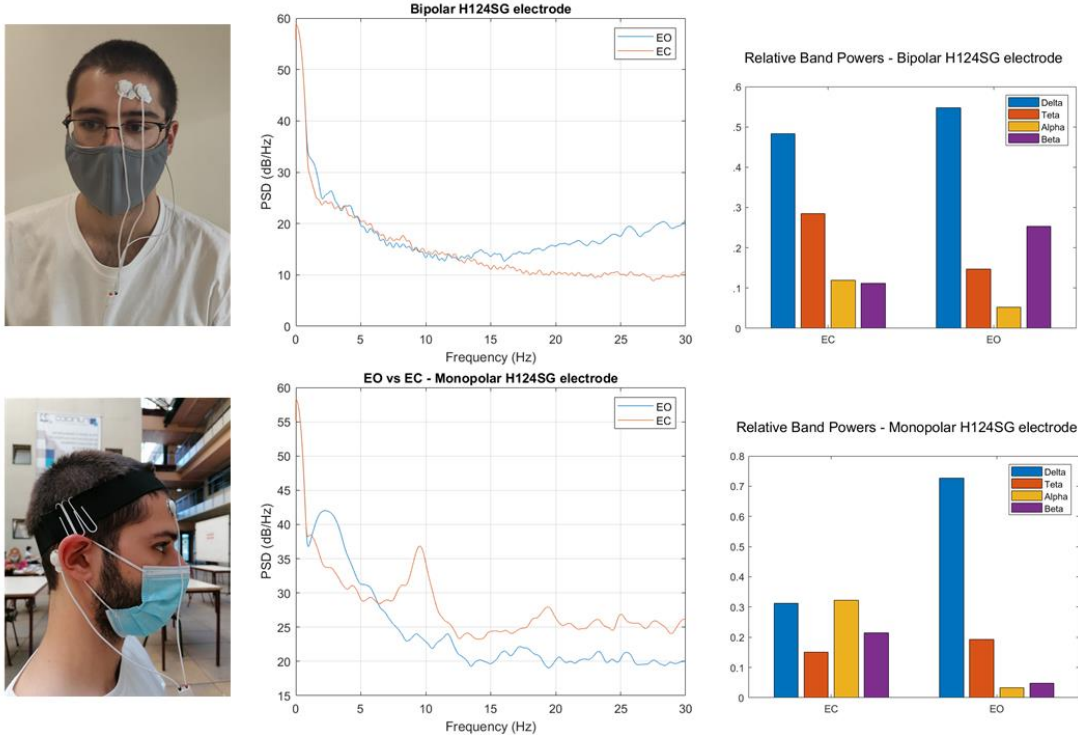


Figure 17 – Comparison between the spectrums and relative band powers of acquisitions during EO and EC in both monopolar and bipolar configurations with a full H124SG electrode montage.

We found that this phenomenon is easily detected in our monopolar acquisitions but not in the bipolar ones. The measured EEG signal is the amplified difference between the two lead electrodes and, as these are located close to each other (less than 3cm as specified in the sensor's documentation []), the variation in alpha power must be similar at both lead's locations thus getting removed along with all other common mode components by the differential amplifier.

Considering all the aspects of the monopolar and bipolar configurations explored above we made decision to opt for a monopolar configuration for our final solution. Despite the drawback of being more susceptible to noise it was this configuration that provided an EEG signal that varied according to the literature. Adding to that, the monopolar configuration is more compatible with the concept of EEG probe as it only requires one electrode as a lead as opposed to the bipolar configuration which would only require two.

Note that we performed acquisitions with other bipolar versions of the monopolar versions we are going to explore in the next section, namely the dry 3D printed electrode bipolar montage and the dry comb Ag-AgCl coated electrode bipolar montage. However, we did not find it relevant to present them in this section as they all depict the same phenomenon observed with the adhesive H124SG electrodes when compared to their monopolar equivalents. These acquisitions are provided in Appendix A for completeness.

3.2 Fixed Configuration Acquisition

Having decided the configuration to be used in our final solution, the next step was to choose the electrodes that were to be employed. For that purpose, we performed acquisitions with various electrodes and electrode combinations.

Gold Cup Electrodes

We started by testing, for reference, how a full gold cup monopolar montage would fair in detecting the increase in alpha power from a EO resting state to an EC as well as in detecting a beta power increase as we transition from a resting state to a more cognitively demanding state (CL). In the next figure we can see the PDS of the acquired EEG signals at every state, as well as the relative band powers.

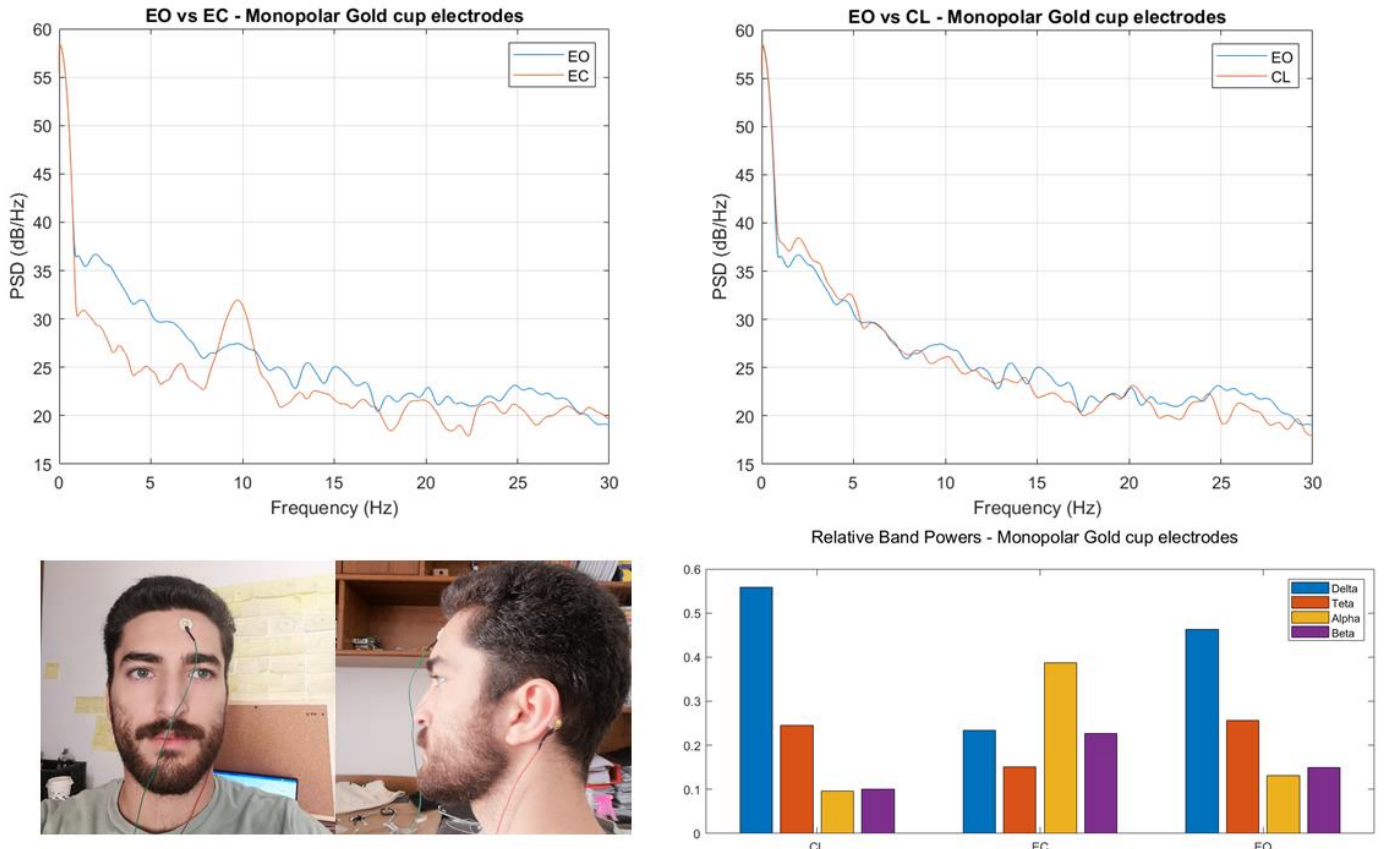


Figure 18 - Comparison between the spectrums and relative band powers of acquisitions during EO and EC with a full monopolar gold cup montage.

We found that this montage accurately detects the increase in alpha power as in the EC state there is a clear peak in the signal's PDS plot at the alpha region. We did not, however, find any relevant variation in beta power from a resting state to a cognitively demanding state. We tried performing the same acquisitions in another subject, but we continued to have no success in detecting said beta power increase. This might be due to a reduced level of focus during the cognitive load task which did not allow the documented rise of this band's power. Alternatively, this beta increase might not be an easily measurable phenomenon in the subjects in question, requiring a more intense cognitive load for it to be detectable. Having this in mind, we opted to solely test the alpha power increase from EO to EC state in further acquisitions, as it is a more well documented phenomenon and significant enough to prove our device's reliability and biological meaning.

H124SG Electrodes

A full H124SG electrode montage was used to perform acquisitions in both EO and EC states and the results are presented below. In the next figures we present the PDS of the acquired EEG signals at both states, the relative band powers and also 10 second low-pass (30Hz) filtered windows of both signals with their respective PDS plots.

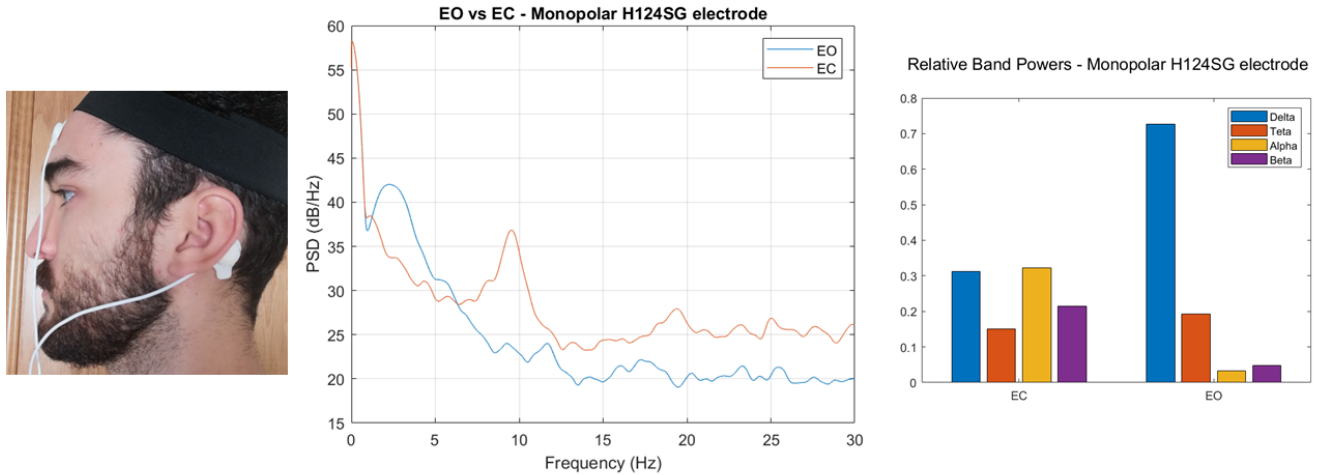


Figure 19 - Comparison between the spectrums and relative band powers of acquisitions during EO and EC with a full H124SG electrode montage.

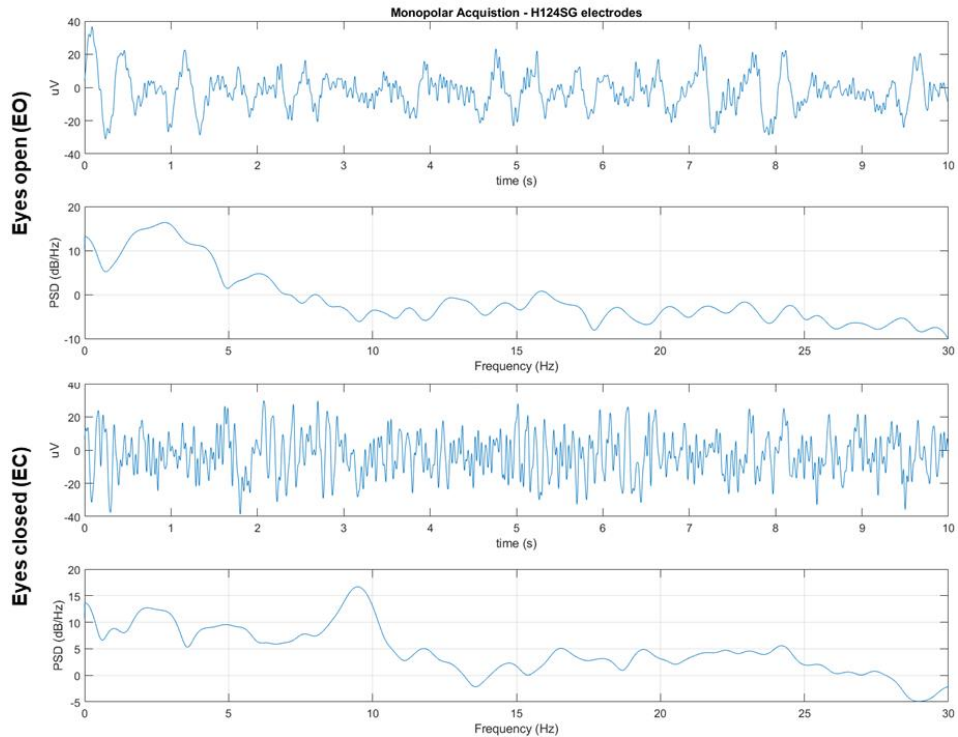


Figure 20 – Ten second windows of low pass filtered EEG signal acquired in EO and EC with full monopolar H124SG electrode montage.

Once more we can clearly identify a peak in the alpha region of the EC acquisition's spectrum, which is not present in the EO acquisition's spectrum. Additionally, in Figure 19 we can observe the differences in

morphology between the signals acquired in each situation. The one acquired during EO varies mostly in slow manner whereas the one acquired during EC varies faster, showing a clear predominance of the alpha range of frequencies. This is a classic behaviour of the EEG.

When comparing the relative powers between the EEG bands within 1-30Hz, we also see that in a eyes open (EO) state we detect larger Delta and Theta powers than in eyes closed state. This comes as the result of the larger amount of eye movement artifacts detected during EO, which are represented by slower variations of the signal and thus are within the Delta and Theta frequency ranges.

Dry comb Ag-AgCl coated Lead and H124SG Reference

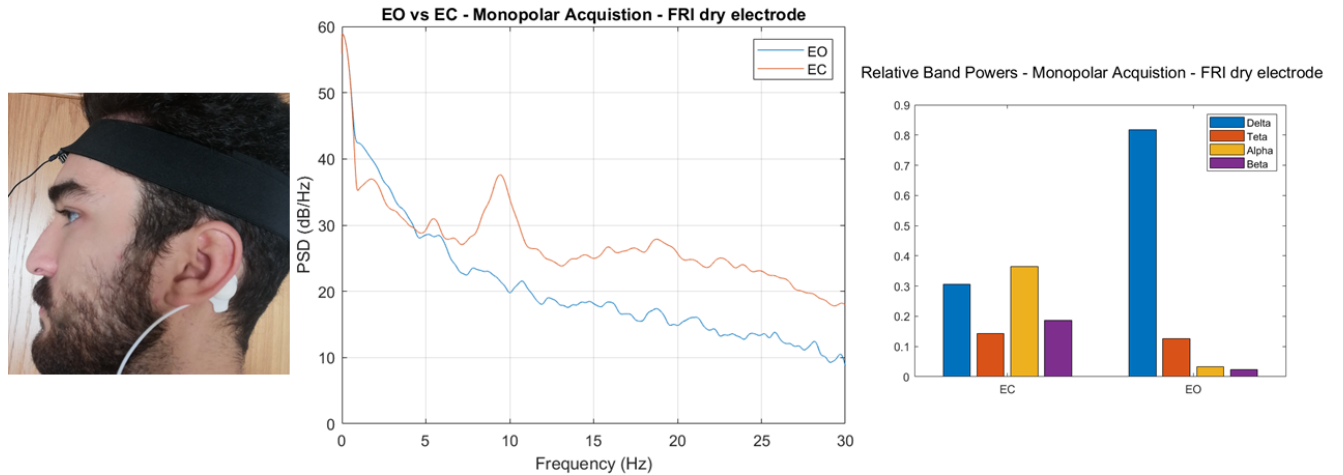


Figure 21 - Comparison between the spectrums and relative band powers of acquisitions during EO and EC with a mixed montage of dry comb Ag-AgCl coated electrode as lead and a H124SG reference electrode

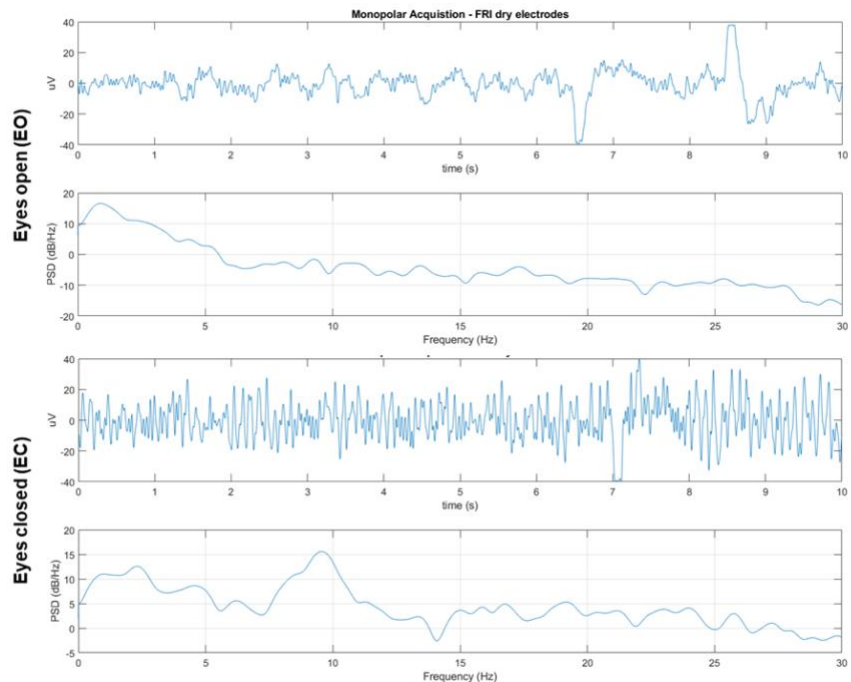


Figure 22 - Ten second windows of low pass filtered EEG signal acquired in EO and EC with a mixed montage of dry comb Ag-AgCl coated electrode as lead and a H124SG reference electrode.

A mixed montage of dry comb Ag-AgCl coated electrode as lead and a H124SG reference electrode was also used to perform acquisitions in both EO and EC states and the results are presented below. In the next figures we present the PDS of the acquired EEG signals at both states, the relative band powers and also 10 second windows of both signals with their respective PDS plots.

This mixed montage is successful in detecting the Alpha power increase from EO state to EC. As it is clear in Figure 21, this leads to a signal that is predominantly varying at frequencies around 10 Hz as opposed to during EO which is when it varies more slowly. Just like in the previous acquisitions we get an increased lower frequency power in EO state when comparing to EC, due to eye movement artifacts. Note that in Figure 22 we can identify the eye blinking artifact as the sudden shift of the signal to more extreme values and later return to the baseline.

This montage, despite being mixed dry, provides the EEG data that is very comparable to wet montages like the one presented in the previous section. Not only it is also able to detect alpha peaks as the overall amplitudes are similar.

Dry Comb 3D Printed Lead and H124SG Reference

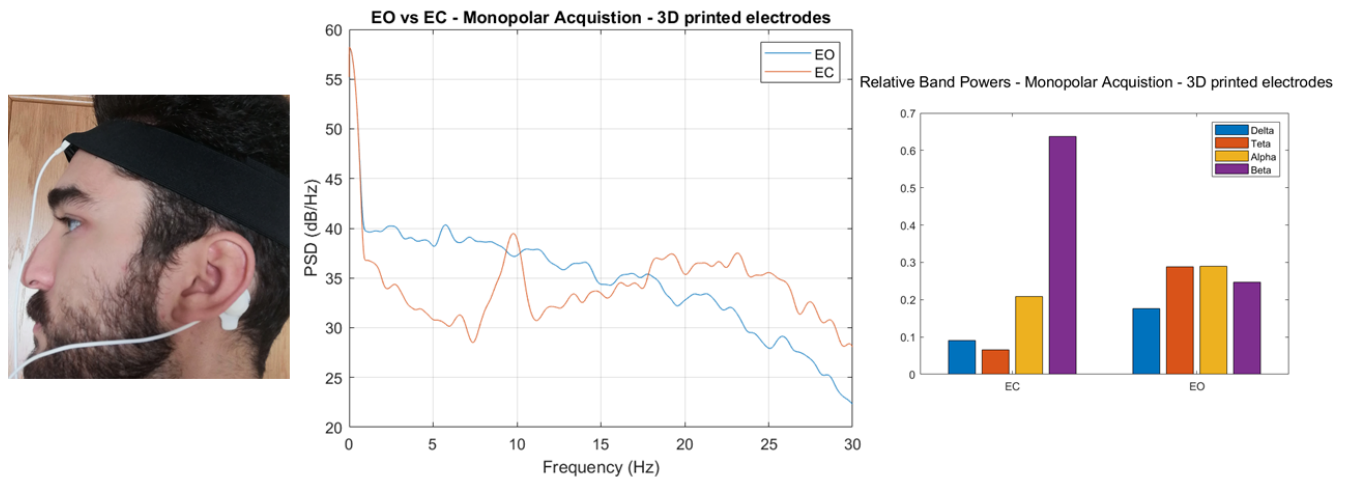


Figure 23 - Comparison between the spectrums and relative band powers of acquisitions during EO and EC with a mixed montage of a 3D printed dry electrode as lead and a H124SG electrode as reference.

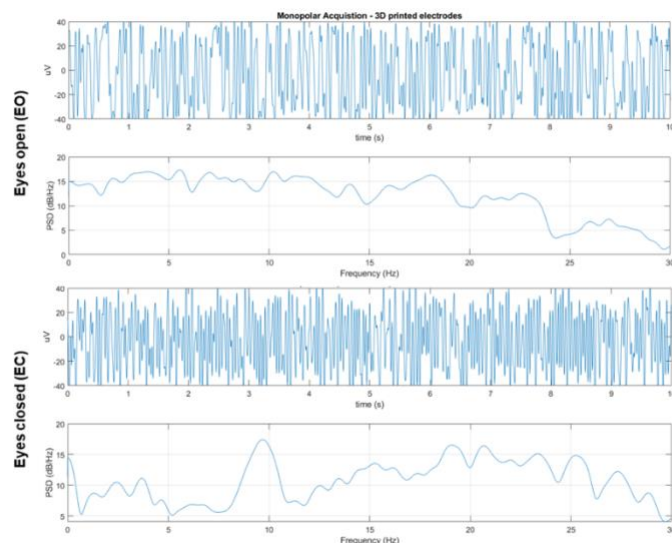


Figure 24 - Ten second windows of low pass filtered EEG signal acquired in EO and EC with a mixed montage of a 3D printed dry electrode as lead and a H124SG electrode as reference.

A mixed montage of one of our 3D printed dry electrodes as lead and a H124SG electrode as reference was also used to perform acquisitions in both EO and EC states and the results are presented below.

It is possible to detect the alpha power increase from one state to another as the peak around 10 Hz is noticeably clear in the EC state's PSD and nonexistent in the EO. However, even though this phenomenon is detectable, there is an unusually intense beta frequency band during EC which is most likely created by noise.

Regarding noise, if we compare the full spectrums of the unfiltered acquisitions from other electrode configurations, we can assess that this montage is the most susceptible to line noise (see Appendix B). Table 2 clearly shows that it is with this montage that we find the largest power at 50 Hz, it being more than twice the powers from the other montages. Note that every acquisition was performed in the same room at virtually equal circumstances.

Since our 3D printed electrodes are estimated to have a significantly larger electrical resistance than the dry comb Ag-AgCl electrodes and the H124SG electrodes, our findings go according the general rule that larger line noise frequency powers are related to larger electrode impedances [17]. Adding to that, we also found a slightly larger line noise frequency power in the montage with the dry comb Ag-AgCl electrode in relation to the one with adhesive wet H124SG electrodes, which also goes according to the abovementioned rule as the dry electrodes have larger electrode impedances than their wet counterparts.

Table 2 - Line noise frequency power at each fixed configuration tested. Obtained from plot in Appendix C.

Type of montage	Power at 50 Hz (dB/Hz)
Full H124SG	8.43
Dry comb Ag-AgCl lead + H124SG reference	9.31
3D printed dry lead + H124SG reference	21.12

Dry Acquisitions at Occipital region

Through the analysis up until now we were able to assess that we could in fact obtain interpretable EEG data through both wet and dry approaches. Ensuring that this was possible was a major step in our project, as we want to guarantee the viability of a dry EEG probe.

With this final objective in mind, we then proceeded to explore how the dry electrode approaches would fair when acquiring signal from the occipital regions of the scalp. This type of acquisition is extra challenging due to the presence of hair, but then again, the comb design of the dry electrodes in use was made to provide a good penetration through hair, maximising contact with the scalp so we should be able to get interpretable EEG data.

Starting by the montage with our 3D printed electrode (Figure 25) we can identify the characteristic EC state alpha peak, however it is heavily overshadowed by an extremely intense beta band. The source of this intense frequency components in the beta range is most likely due to external noise as this power levels cannot be physiologically explained. In the EO acquisition we find a similar shaped interference that is shifted for higher frequencies, closer to the line noise frequency.

Even though we can detect the alpha peaks at the EC the general predominance of alpha waves in this occipital region at all states cannot be identified, as there is extensive corruption by beta frequency range components.

This worse performance is most likely explained by bad contact between the electrode and the scalp, which in this case is made extra difficult due the existence of dense hair. Despite this electrode's design having a total of 11 pins to enable good hair penetration, we find that in locations with very dense hair the width of the pins might be

too large to allow a good contact with the scalp, thereby leading to an even higher electrode-scalp interface impedance.

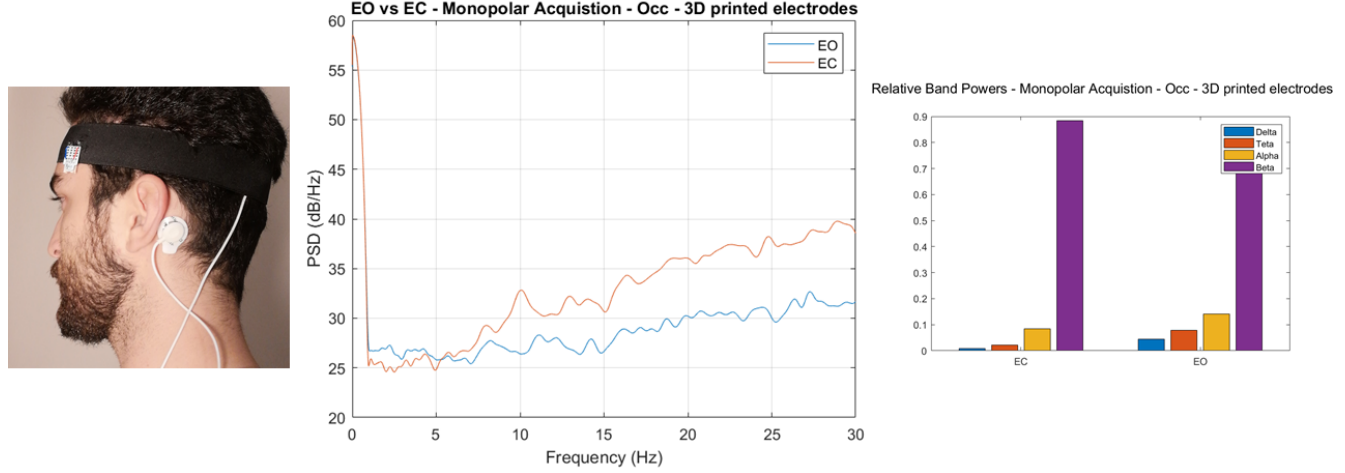


Figure 25 - Comparison between the spectrums and relative band powers of acquisitions during EO and EC with a mixed montage of a 3D printed dry electrode as lead and a H124SG electrode as reference at the Occipital region.

As opposed to the configuration using the 3D printed electrodes, the one with the dry comb Ag-AgCl coated ones allows the identification of not only the generally more intense alpha rhythms at both states when compared to frontal acquisitions, but also the characteristic alpha power increase in EC state.

When comparing with the previous configuration, this better performance can be explained by a superior electrode design, with thinner pins allowing better hair penetration and scalp contact, which lead to a minimisation of the electrode-scalp interface impedance.

Note that it is possible to consult the raw EEG signal obtained from this configuration and the previous at the occipital region in the Appendix C.

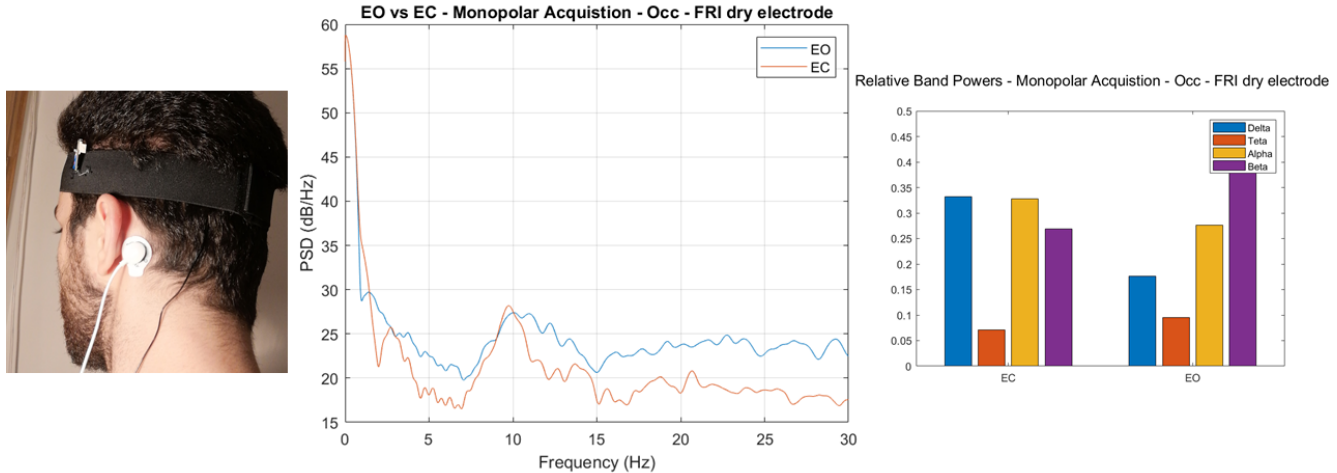


Figure 26 - Comparison between the spectrums and relative band powers of acquisitions during EO and EC with a mixed montage of dry comb Ag-AgCl coated electrode as lead and a H124SG reference electrode at the Occipital region.

Inter-subject variability

During our acquisitions we were able to consistently detect that Subject 1 presented a more evident increase in alpha power during EC than Subject 2. In fact, acquisitions on Subject 2 most of the times did not even succeed to present any measurable difference in alpha power between EO and EC (see Figure X). We can suppose that this stems from a general difficulty of this subject to reach a state of eyes closed relaxation required for this experiment. Another plausible explanation is that it might be a characteristic of this subject's EEG data to not depict the alpha increase in EC at frontal regions of the head.

Note that given this situation the EEG data presented in the previous and following sections were obtained mostly from Subject 1.

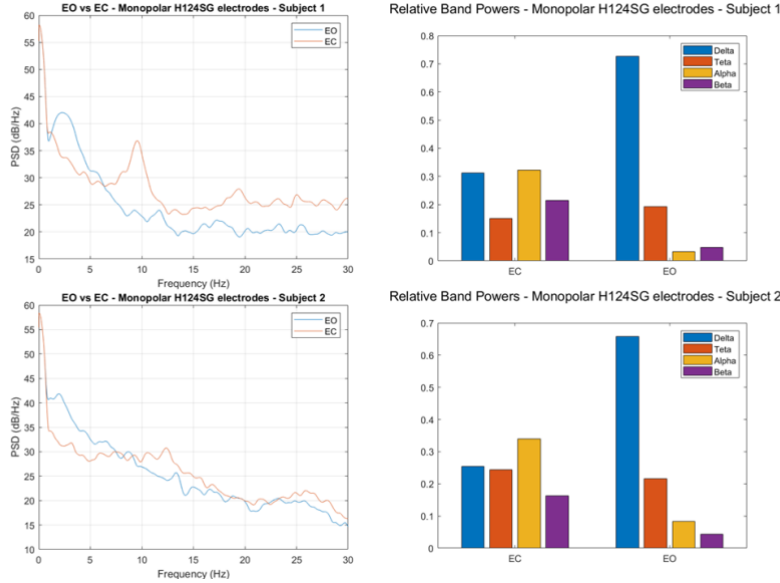


Figure 27 - Comparison between the spectrums and relative band powers of acquisitions during EO and EC with a full H124SG electrode montage from Subject 1 and 2.

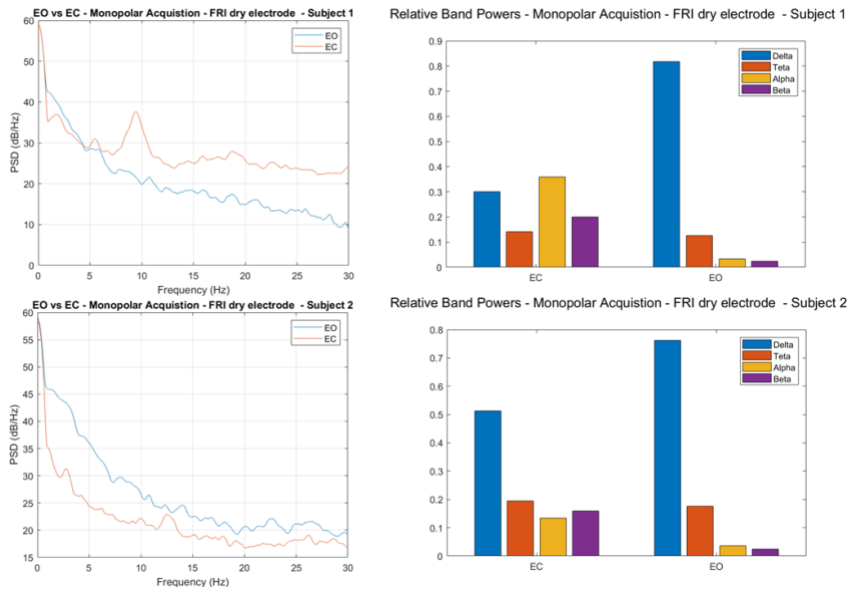


Figure 28 - Comparison between the spectrums and relative band powers of acquisitions during EO and EC with mixed montage of dry comb Ag-AgCl coated electrode as lead and a H124SG reference electrode montage from Subject 1 and 2.

3.3 Hand-held Probe Acquisition

The solution encountered for the final iteration of the probe allow to switch between two conformations with either our own 3D printed electrodes or the dry comb AgCl. The measurements were made by the own subject of the study in question, while trying to stabilize the probe. This non-fixed nature of the device is one of its main aspects but also challenges since the quality of the signal can be heavily affected by the handling and placing of the probe. And so, the goal of these tests was to assess whether a signal of acceptable quality could be obtained. Since the tested electrodes were dry, they were also tested in the occipital region since their fixation isn't an obstacle anymore.

In Figure 29 we can see the full waves of the signals acquired with the dry comb AgCl coated electrode conformation placed on the forehead both for eyes closed and eyes closed as well as a 10 second section of the signal, with also their respective power density spectrums.

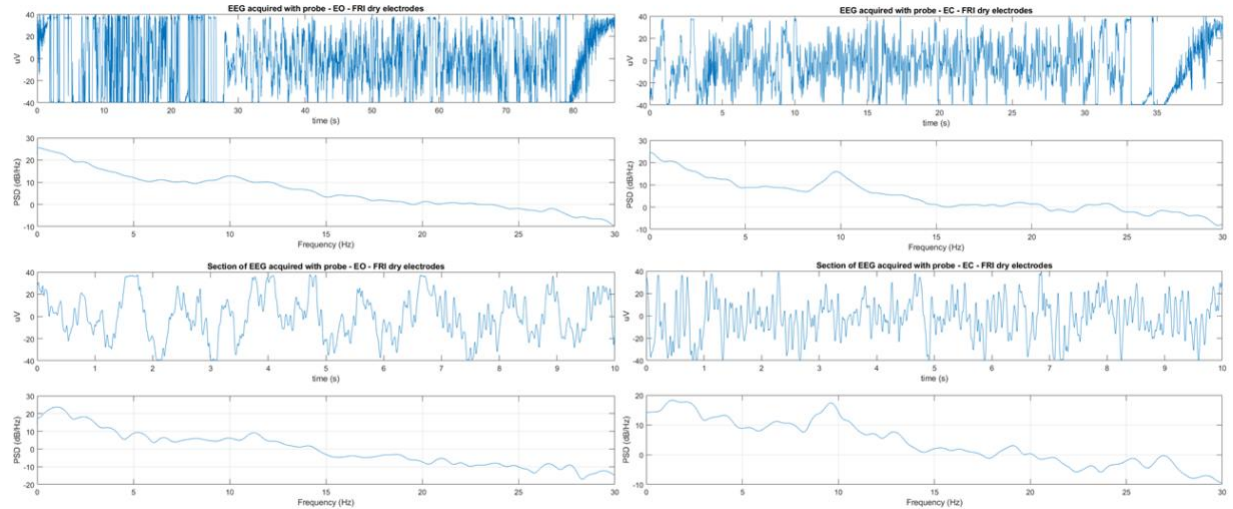


Figure 29 – EEG signal for eyes open (left) and eyes closed (right) with probe placed on frontal region, with respective PDS plots and also 10 second sections with also PDS.

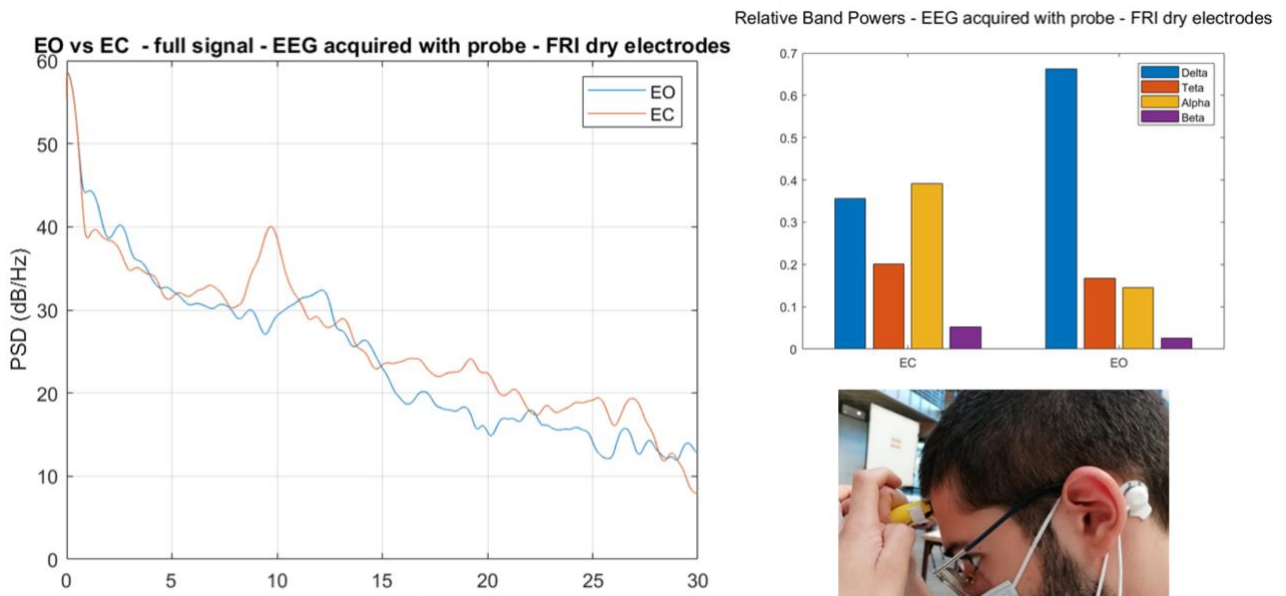


Figure 30 – Comparison of PDS plots (left) and band densities (upper right). Demonstration of experimental acquisition (lower right).

Looking first at the plots of the signal it is visible that they can be heavily corrupted by noise or by artifacts of motion due to imperfect stabilization of the hand, mainly in the first 30 seconds of the eyes open signal and at the end of the eyes open acquisition. Still, despite this, there is a clear peak in the alpha bandwidth when the eyes are closed, as expected. When confining the analysis to only 10 seconds of good quality signal, the behaviour of the PDS plots remains similar. The relative band powers in Figure X also illustrate this, with a visible increase of alpha in EC.

Next are presented the results for the 3D printed electrodes on the frontal region.

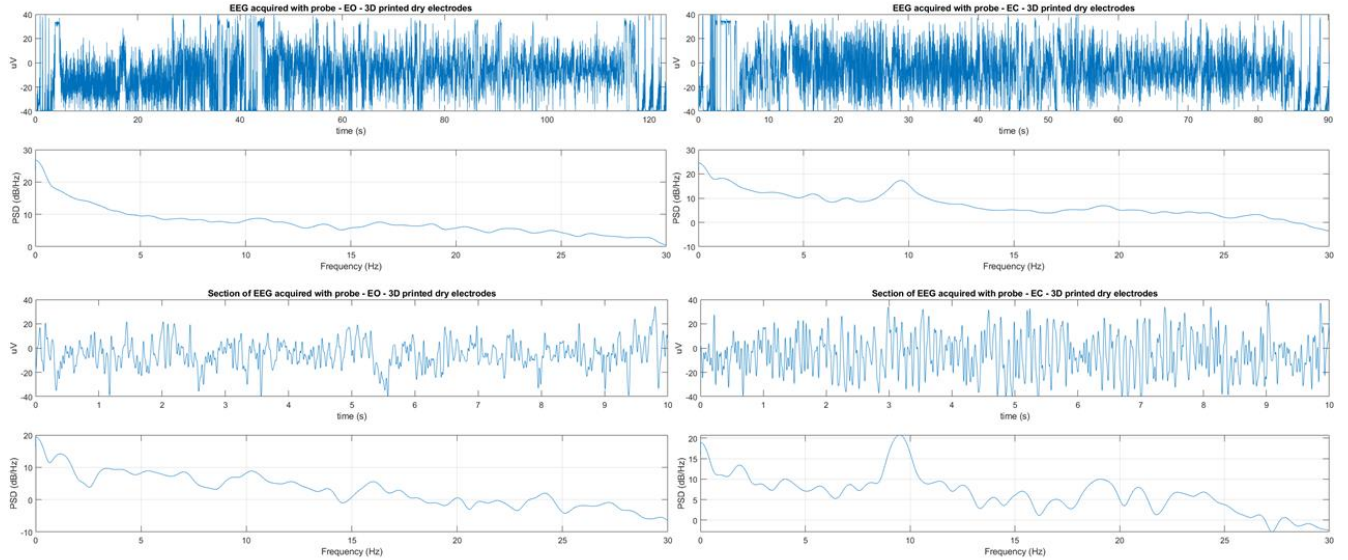


Figure 31 - EEG signal for eyes open (left) and eyes closed (right) with probe placed on frontal region, with respective PDS plots and also 10 second sections with also PDS.

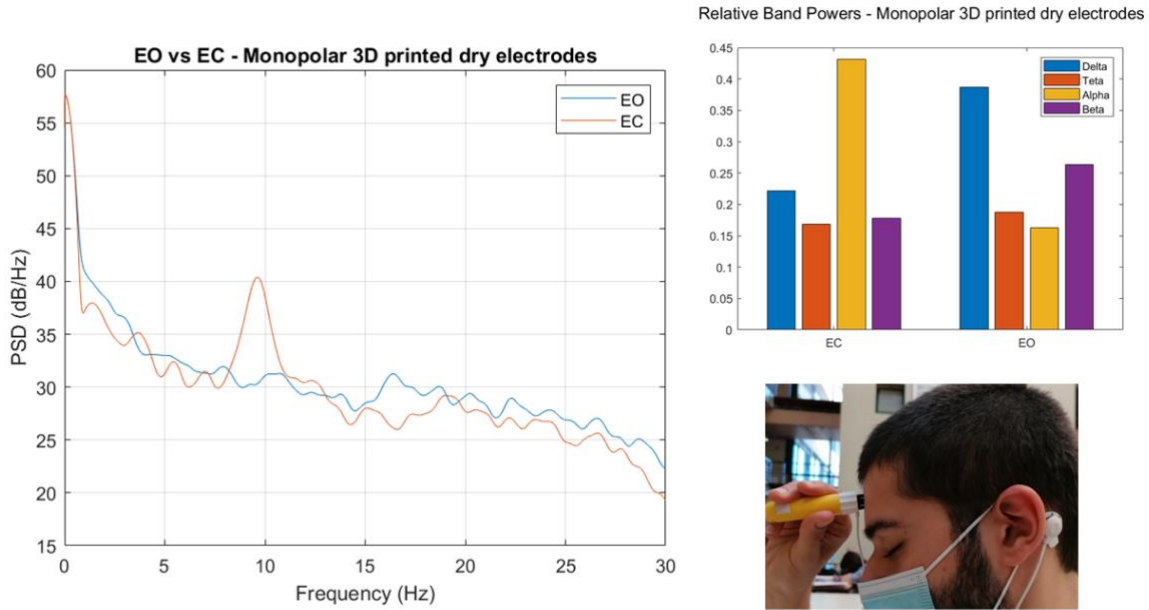


Figure 32 - Comparison of PDS plots (left) and band densities (upper right). Demonstration of experimental acquisition (lower right).

The results are similar to those obtained with the other electrodes, except this signal isn't influenced as much by the electrical supply noise. Lower frequencies are less prominent, as shown by the relative band powers in Figure X. The peak on the alpha band in EC is also more pronounced with the relative band powers maintaining their values.

Next, acquisitions were made in the occipital region. In the following figures are represented the results with the AgCl dry comb electrodes.

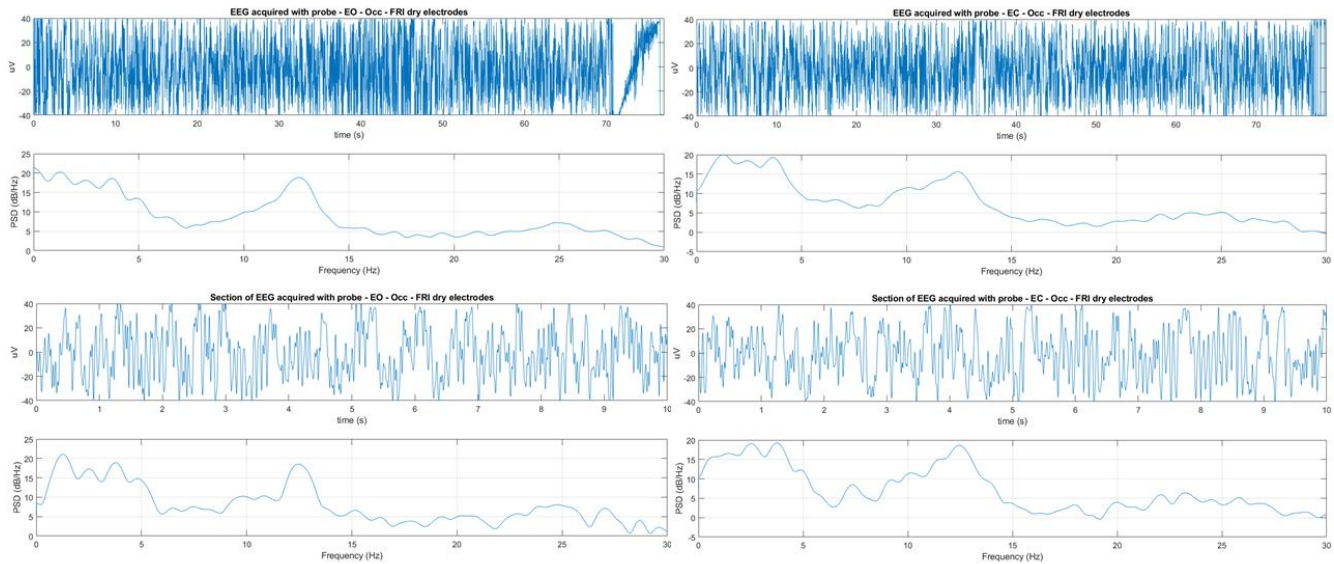


Figure 33 - EEG signal for eyes open (left) and eyes closed (right) with probe placed on the occipital region, with respective PDS plots and also 10 second sections with also PDS.

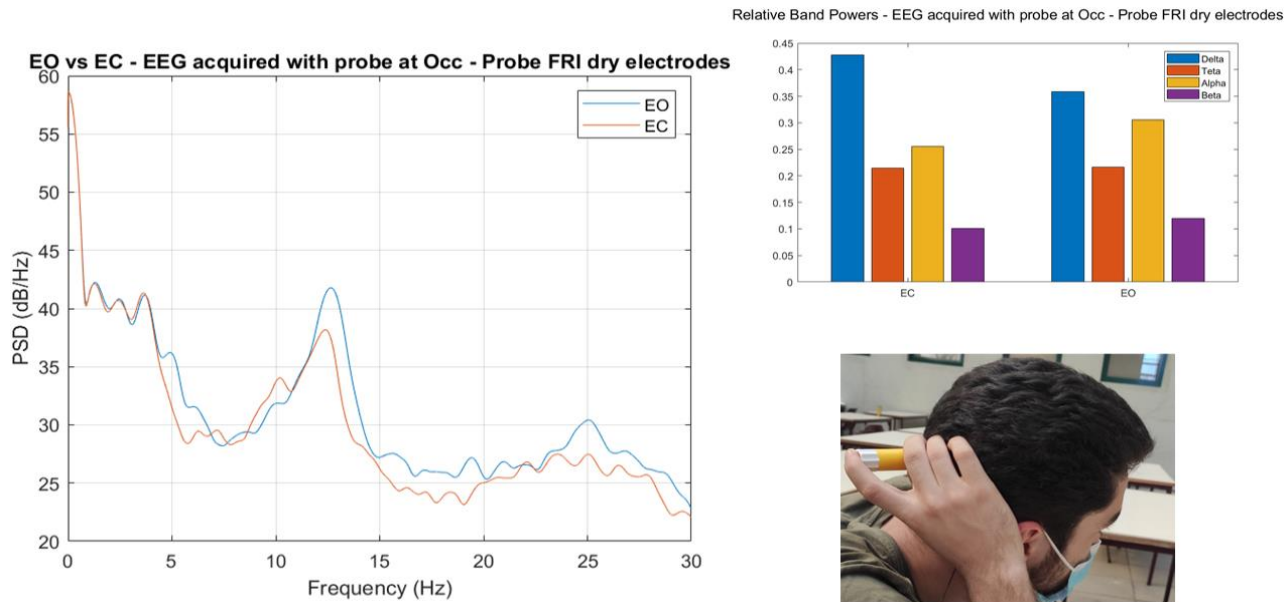


Figure 34 - Comparison of PDS plots (left) and band densities (upper right). Demonstration of experimental acquisition (lower right).

In this case, the first thing that stands out are the clear peaks in the alpha band in both situations EC and EO. This is expected since the occipital region usually displays a higher activity in this band. Another thing is that there is not a distinction in the power density spectrums between both situations. This can be due to the influence of the hair, which can corrupt the signal as well as a more difficult stabilization of the probe in this configuration.

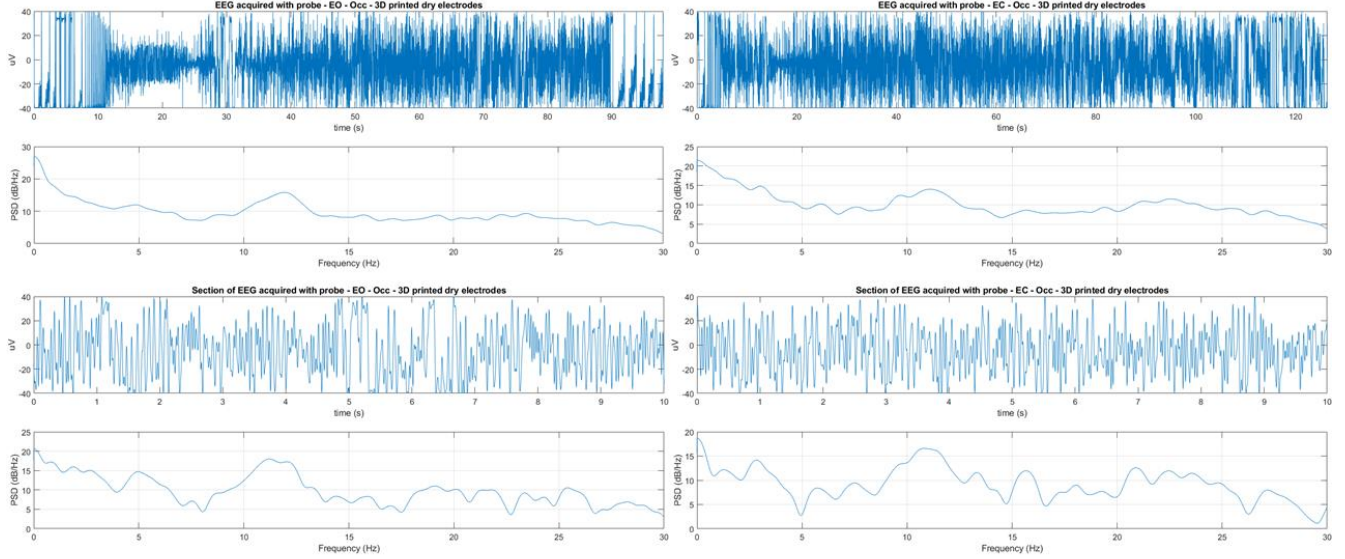


Figure 35 - EEG signal for eyes open (left) and eyes closed (right) with probe placed on the occipital region, with respective PDS plots and also 10 second sections with also PDS.

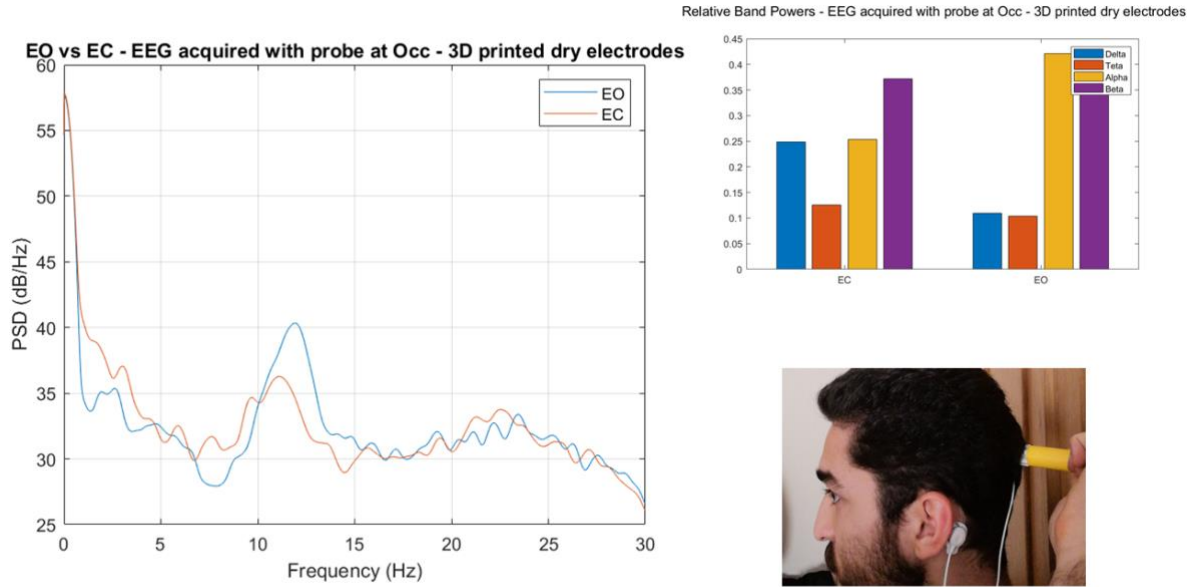


Figure 36 - Comparison of PDS plots (left) and band densities (upper right). Demonstration of experimental acquisition (lower right).

In what concerns the 3D printed electrodes, the distinction between EC and EO is also difficult but with the peaks in both situations being visible, although not as pronounced as with the AgCl coated ones. This can be due to the electrodes design. They are bigger which leads to them not being able to penetrate the hair as easily, resulting in an attenuation of the signal. The measurements with the probe are also prone to slight variability between the

location of successive acquisitions due to its handheld mobile nature, a problem that is not present in the fixed configuration measurements. This can be one of the sources error that lead to the unexpected results seen above.

4 Final Remarks

As first comment, our results allow us to prove the effectiveness of our pipeline, in particular from the sensor to the real time processing and display, in the acquisition of EEG.

Considering our results, we find that, provided that we are in an environment with minimal power line noise, this single channel EEG probe can indeed provide interpretable EEG data, depicting well documented alpha power increases from EO to EC and from the frontal region to occipital regions. The most suitable type of electrode configuration to be used in our probe was found to be the dry comb Ag-AgCl lead with the H124SG reference. The wet adhesive reference allows good fixation while also being minimally uncomfortable. Despite being slightly more susceptible to noise than the one used for reference, the lead electrode is still quite resilient to it, due to low electrode impedance provided by its very conductive coating. Its design is also an advantage as the thin pins provide a good contact with the scalp even in locations with dense hair. On that note, the 3D printed dry comb electrodes are not so resilient to noise mainly due to their larger electrical resistivity provided by the PLA, which is less conductive than the coating used in the ones mentioned previously. We found that its design is also suboptimal as the thicker pins and larger size do not provide such good hair penetration and scalp contact as the other dry comb electrode.

The hand-held probe acquisitions present an extra challenge due to the stabilization of the lead electrode being dependent of the examiner's grip. This makes for an EEG signal that is more susceptible to noise due to larger electrode-scalp interface impedance at times. To make our device suitable even for examiners with unstable grips, we include in our final design an elastic band that can be used to perform more stable acquisitions.

What was also made clear with our analysis is that, provided that we are in an environment with minimal power line noise, both types of dry electrodes allow the acquisition of EEG signal whose shape is recognisable and similar to what is depicted in the literature. This is a relevant achievement as, according to the literature and also made clear during our meeting with Dra. Ana Rita Peralta, the diagnosis of epileptic seizures relies mostly on the detection of extreme variations of EEG signal, which we find our device to be able to detect.

Due to time restriction, we were not able to explore and develop our device as much as we wanted to, therefore we are leaving some suggestions for our final solution that can be implemented in the future. Starting by the 3D printed electrodes, it would be relevant to design one version of these electrodes that is smaller in size, having thinner pins with slightly sharper endings, with view of improving the electrode-scalp interface impedance. It would also be interesting to implement a more user-friendly interface, allowing an even easier usage of our device by health professionals as pre-screening tools.

References

- [1] D. L. Schomer and F. H. Lopes da Silva, *Niedermeyer's Electroencephalography*, vol. 1, no. 9. Oxford University Press, 2017.
- [2] O. Mecarelli, *Clinical Electroencephalography*. Cham: Springer International Publishing, 2019.
- [3] F. Grosselin *et al.*, "Quality assessment of single-channel EEG for wearable devices," *Sensors (Switzerland)*, vol. 19, no. 3, pp. 1–17, 2019, doi: 10.3390/s19030601.
- [4] S. Krachunov and A. J. Casson, "3D Printed Dry EEG Electrodes," *Sensors (Basel)*., vol. 16, no. 10, 2016, doi: 10.3390/s16101635.

- [5] J. W. Y. Kam *et al.*, “Systematic comparison between a wireless EEG system with dry electrodes and a wired EEG system with wet electrodes,” *Neuroimage*, vol. 184, no. September 2018, pp. 119–129, 2019, doi: 10.1016/j.neuroimage.2018.09.012.
- [6] F. Pinho, J. Cerqueira, J. Correia, N. Sousa, and N. Dias, “myBrain: a novel EEG embedded system for epilepsy monitoring,” *J. Med. Eng. Technol.*, vol. 41, no. 7, pp. 564–585, 2017, doi: 10.1080/03091902.2017.1382585.
- [7] L. G. Fehmi and T. Collura, “Effects of Electrode Placement Upon EEG Biofeedback Training: The Monopolar-Bipolar Controversy,” *J. Neurother.*, vol. 11, no. 2, pp. 45–63, Jul. 2007, doi: 10.1300/J184v11n02_04.
- [8] “Bluetooth Mate Silver.” https://www.ptrobotics.com/modulos-bluetooth/1444-bluetooth-mate-silver.html?gclid=Cj0KCQjwnueFBhChARIsAPu3YkQ1Ok5a8U5EELHz9WUSO_bigIMrMQC5gLET2PNw9iFpULcaWToaA0aArYzEALw_wcB (accessed Jun. 10, 2021).
- [9] A. C. Metting van Rijn, A. Peper, and C. A. Grimbergen, “High-quality recording of bioelectric events,” *Med. Biol. Eng. Comput.*, vol. 29, no. 4, pp. 433–440, Jul. 1991, doi: 10.1007/BF02441666.
- [10] “Electroencephalography (EEG) Sensor.” <https://plux.info/sensors/12-electroencephalography-eeg-sensor.html> (accessed Jun. 10, 2021).
- [11] “EEG Gold Cup Electrodes Package with 1.5 DIN Plug Assorted Colors Package.” <https://www.fri-fl-shop.com/product/eeg-gold-cup-electrodes-package-with-1-5-din-plug-assorted-colors-package-choose-quantity-length/> (accessed Jun. 10, 2021).
- [12] “Covidien Kendall Disposable Surface EMG/ECG/EKG Electrodes 1” (24mm) 50pkg.” <https://biomedical.com/covidien-kendall-disposable-surface-emg-ecg-ekg-electrodes-1-24mm-50pkg.html> (accessed Jun. 10, 2021).
- [13] “TD-244 Ten20 EEG Adhesive Paste.” <https://www.fri-fl-shop.com/product/td-244-eeg-adhesive-paste/> (accessed Jun. 10, 2021).
- [14] “Conductive PLA.” <https://www.proto-pasta.com/pages/conductive-pla/> (accessed Jun. 10, 2021).
- [15] “The McGill Physiology Virtual Lab - Biomedical Signals Acquisition, EEG.” https://www.medicine.mcgill.ca/physio/vlab/biomed_signals/eeg_n.htm (accessed Jun. 10, 2021).
- [16] “New Longer 5mm Spike disposable/reusable dry EEG Electrode TDE 210.” <https://www.fri-fl-shop.com/product/new-longer-5mm-spike-disposable-reusable-dry-eeg-electrode-tde-210/> (accessed Jun. 10, 2021).
- [17] E. S. Kappenman and S. J. Luck, “The effects of electrode impedance on data quality and statistical significance in ERP recordings,” *Psychophysiology*, Mar. 2010, doi: 10.1111/j.1469-8986.2010.01009.x.

Appendix A – Bipolar Acquisitions

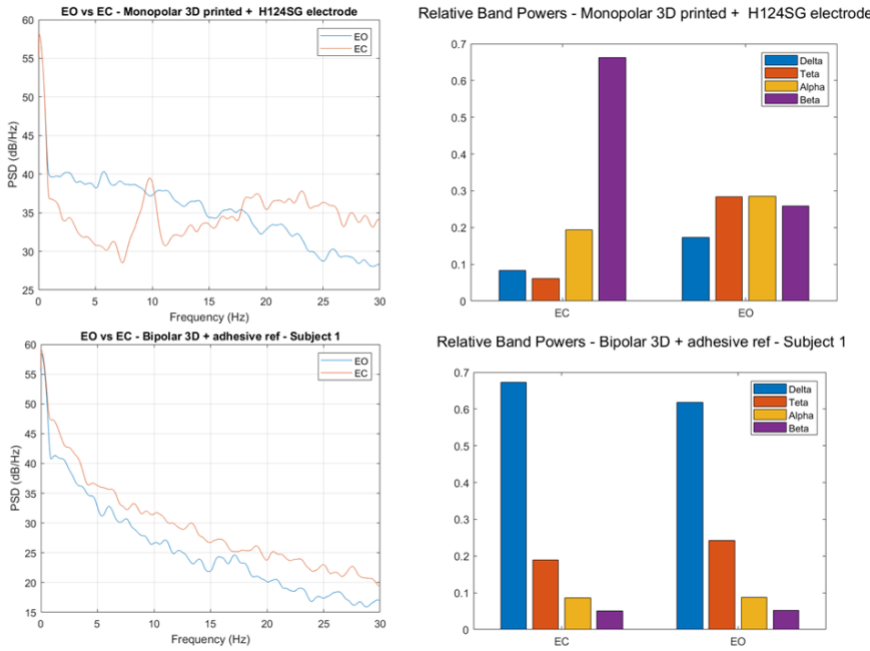


Figure 37 - Comparison between the spectrums and relative band powers of acquisitions during EO and EC in both monopolar and bipolar configurations with a mixed 3D printed electrode montage.

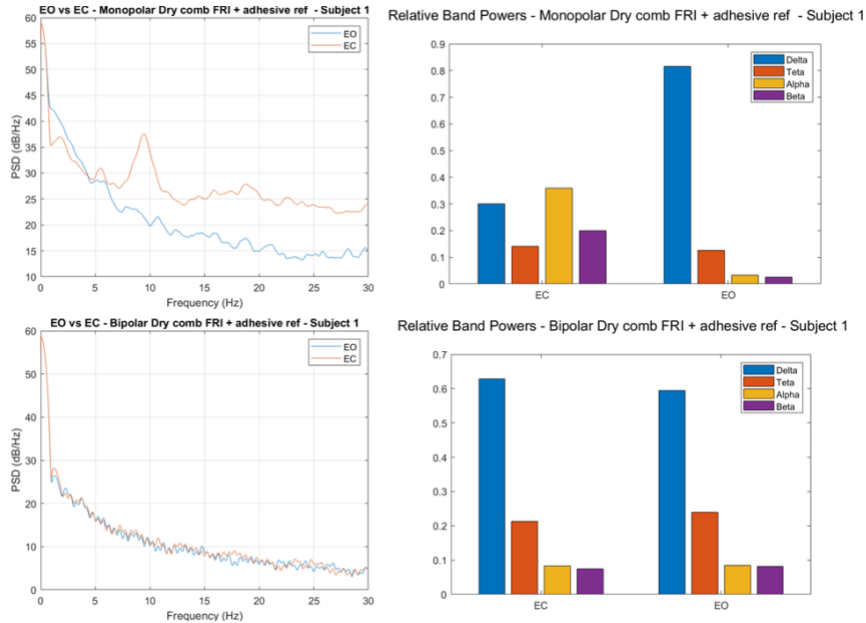


Figure 38 - Comparison between the spectrums and relative band powers of acquisitions during EO and EC in both monopolar and bipolar configurations with a mixed dry comb coated electrode montage.

Appendix B – Electrode noise susceptibility

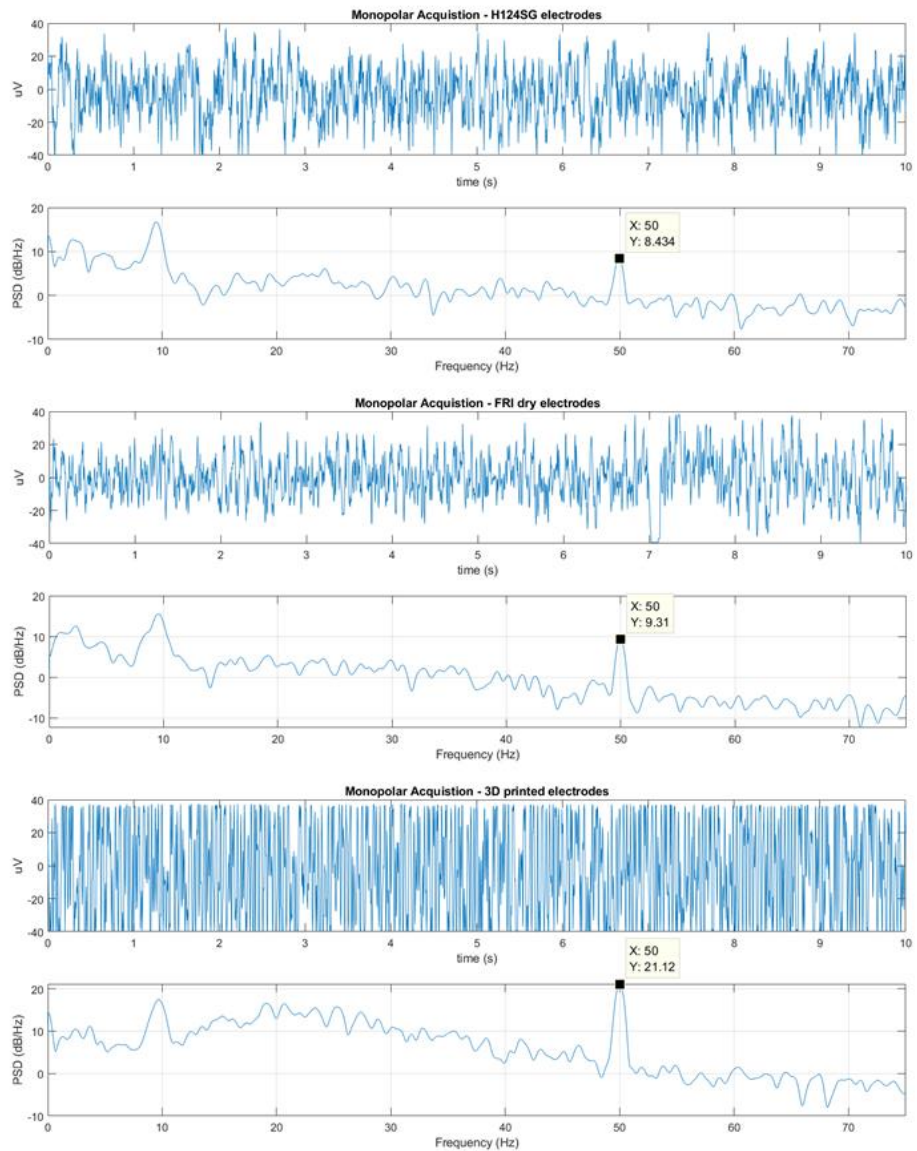


Figure 39 - Comparison of line noise susceptibility through plots of ten second windows of the acquired EEG signal with each type of electrode. (top) Adhesive electrodes; (middle) Dry comb coated electrode; (bottom) 3d printed electrodes.

Appendix C – Fixed Dry Acquisition at Occipital region

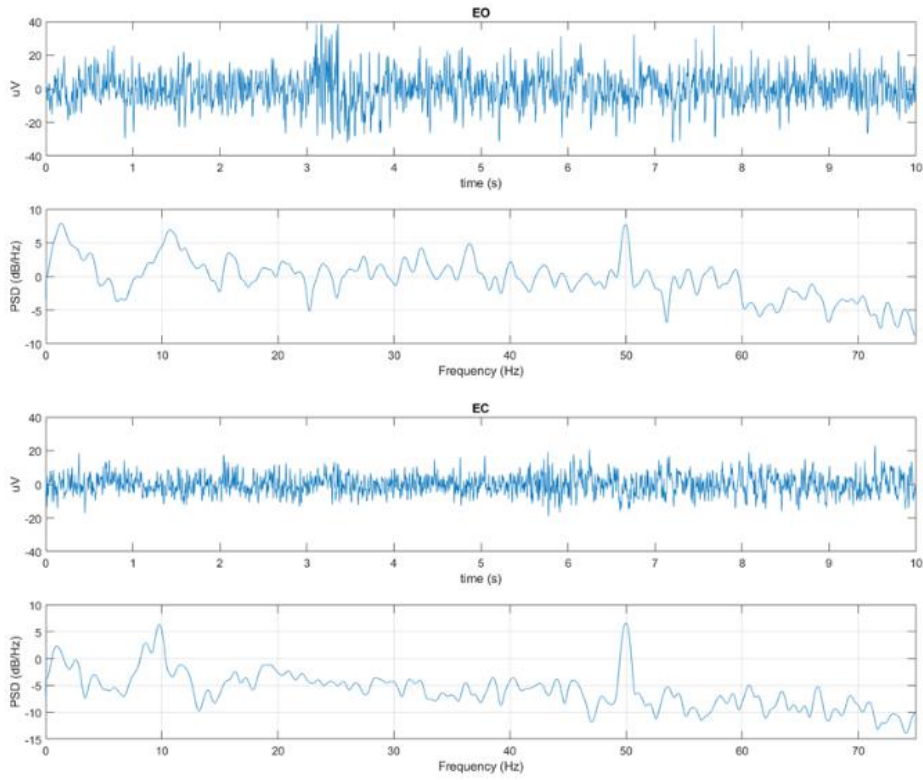


Figure 40 – Ten second window of raw EEG signal acquired at the Occipital region through the montage with the dry comb coated electrode.

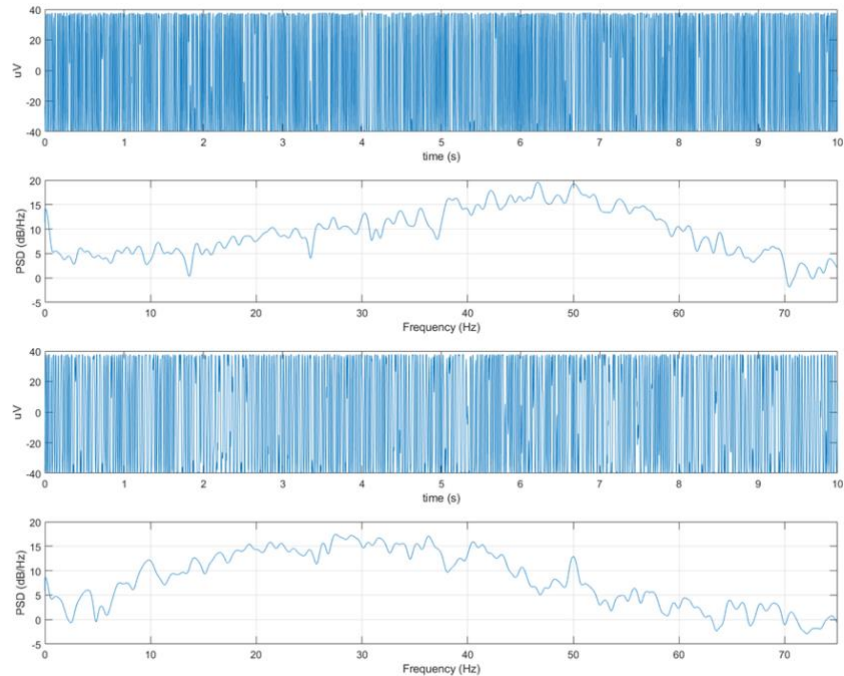


Figure 41 – Ten second window of raw EEG signal acquired at the Occipital region through the montage with the dry comb 3D printed electrode.